Electron transport in Silicon Carbide system

Roba Chukalo

A Thesis submitted to
The Department of Physics

In Partial fulfilment of the Requirements for the
Degree of Master of Science (Physics)

Addis Ababa University
Addis Ababa, Ethiopia
January 2020

Addis Ababa University
College of Natural Sciences
School of Graduate Studies

This is to certify that the thesis prepared by Roba Chukalo entitled: *Electron transport in SiC system* and submitted in partial fulfilment of the requirements for the Degree of Master of Science complies with the regulations of the University and meets the accepted standards with respect to originality and quality.

Signed by the Examining Committee:

Examiners

1. Dr. Lemi Demeyu Signature ..... Date .....

2. Dr. Yitagesu Elfagd Signature ..... Date .....

Advisor(s)

1. Dr. Kenate Nemera Signature ..... Date .....

Chair of Department or Graduate Program Coordinator

Abstract

In this work electron transport in silicon carbide (SiC) system were considered. The calculations are done based on Density Functional Theory (DFT) which adopt a use of the generalized gradient approximation (GGA) in PBE. An abinit code based on the DFT is applied. From the calculations, we obtained optimum values of lattice constant (parameters), bulk modulus, cut-off energy, and different energies (surface energy, cohesive energy, vacancy energy) of silicon carbide. These results are reported using a step-by-step approach and compared with other exprimental values. Analysis based on bandstructure, density of state, projected density of state, work-function, and optical properties are also presented. The optical property has a direct relationship with the distribution of crystal bandgap and electronic density of state. The Monte Carlo method takes into account band structure model to investigate electron transport.

Keyword: Silicon Caribide (SiC), DFT, GGA, ABINIT, MC, Electron transport, bandstructure, DOS, PDOS, optical properity, and workfunction.

Acknowledgment

First of all I would like to thank to my Almighty **God** for giving me health, strength and for hope that keeps my believing that this affiliation would be possible and more interesting. Next to this, I express many greatest gratitude and special thanks to **Dr. Kenate Nemera** for giving me the opportunity to study and work on a very interesting topic. And also I appriciate him for his invaluable assistance, patience, useful suggestion, continuous guidance, constructive criticisms, encouragement, whole hearted supervision and support throughout the progress of my work. I am also very greateful to **Dr. Lemi Demeyu** for providing the statistical probability of particles and the basic concept of Monte-Carlo simple sampling method of integration.
And also I would like to thanks all the physics department members/staff that always kindly proved me with necessary assistance and for their scientific advice, many suggestion and friendly help.
I would also greately indebted to thanks **South Nation-Nationality and People Represtative (SNNPR) educational bureau** for its sponsorship to attend this master degree program in Addis Ababa University.
Finally, I would like to thank all the support from my family especially my parents during my life and also my wife Amarech Alemu Fola as a M.Sc students. With out their support it could not be possible for me to continue my academic career.

Contents

List of Figures

List of Tables

Preface

This work is dedicated to: I am deeply greateful to my father Ato Chukalo Chucho and my mother w/ro Kole(Ayelech) Elicho in addition to my wife Amharech Alemu with son's Kalikidan Roba, Nebiyou Roba and Anjonyo Roba for your constant and always loving support to my work. This M.Sc graduate thesis paper is dedicted to you.

Chapter 1

Introduction

1.1 Motivation and Backgroud of silicon carbide

Silicon carbide is a very promising semiconductor material for high temperature, high frequency, and high power applications. The invention of silicon carbide (SiC) goes back to 1893, when E.G. Acheson [1] Patented a method for making the powder. It has been used as an abrasive and cutting tool until 1907, when the first SiC light emitting diode (LED) was discovered by H.J.Round [2]. The difficulty of crystal properties, and purity, to some extent, was solved by Lely's methods, in which SiC powder is evaporated at elevated temperature in graphite crucible, and then sublimes on porous graphite wall inside the crucible, forming hexagonal platelets [3]. In 1978, Tairov, and Tsvetkov introduced the seeded sublimation method, as physical vapor transport, to have better control the polytypes by spontaneous nucleation on the graphite walls. Nowadays, 4H-SiC and 6H-SiC Wafers of several inches in diameter are available commercially by modified physical vapor transport, several groups world wide have the ability of making high quality SiC Wafers [4]-[6] and steps controlled epitaxy [6].

1.2 Crystal structure for SiC

Silicon carbide is a wide band-gap semiconductor with high breaking voltage and high saturation electron drift velocity (v_d). It is the only semiconductor material that exhibits a wide range polytypes. Silicon carbide has over 200 different polytypes, different possible stacking arrangements. One of the most useful forms of Silicon carbide is 3C-SiC, or β-SiC, being the only silicon carbide polytype having the diamond-like Zinc-blend Structure and also it has B3-structure. Among all SiC polytypes 3C-SiC, 4H-SiC and 6H-SiC polytypes are attracting more attention because of the favorable electronic properties. It composed of carbon and silicon in a stoichiometric ratio of 1:1. Each atom is bonded to four atoms of the other elements. They all have common building blocks: the Si-C tetrahedron [7].
Silicon: Silicon has 14 electrons. Ten of them will be found in the 1s,2s and 2p orbitals close to the nucleus, the next two going into the 3s orbital. The remaining ones will be in two separate 3p orbitals. The electronic structure of silicon is written in the form $1s^2 2s^2 2p^6 3s^2 3p^2$. Because of this configuration, Si atoms most frequently establish sp^3 bonds (hybridization of a s orbital and three p orbitals)

leading to tetrahedrally coordinated phases [8].
Carbon: Carbon has six electrons. Two of them will be found in the 1s orbital close to the nucleus forming a compact core, the next two going into the 2s orbital. The remaining ones will be in two separate 2p orbitals. The electronic structure of carbon is normally written $1s^2 2s^2 2p^2$. Hence, of this configuration, C atoms frequntily estabilish sp^3 bonds hybridization in cubic diamond carbon.

1.3 Importances of silicon carbide

The advantages of the three most stable SiC polytypes brought a boost and stronger interest for electrical devices in high-temperature, high-power and high-voltage applications such as: computer and cell-phones industry, motor and traction control, smart power grid, electrical vehicles, power converters for renewable energies, energy storage, naval power system, solar cells, medical and biotechnology, harsh environment sensors [9]. SiC material is also known as a biocompatible material that can be used for biochemical or medical sensors. It has been reported the use of SiC material as hard coating for numerous biomedical applications: non-fouling coatings on coronary heart stents and/or a passivation layer for prosthetic bone implants [10]. Moreover, SiC material found its use as nuclear fuel particle coatings in Nuclear Power Plants. It is thus increasingly clear that SiC electronic systems will dominate the new energy and **electron transport technologies** of the 21st century. Many different polytypes have been identified so far [11], but only 3C, and the hexagonal 4H, and 6H have the most technological importance. Although the chemical compound and the building block of all the polytypes are the same Si-C tetrahedron, their stacking sequences are varied. Crystal structural model for SiC is showing as follows:

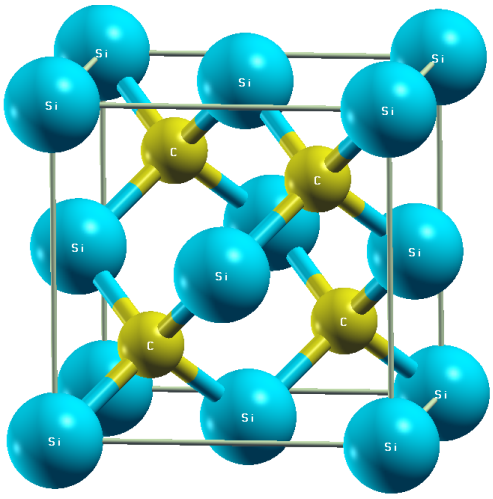

Figure 1.1: Crystal structural model for SiC (zinc blende SiC) by (xcrysden) in this work.

This crystal structure belongs to cubic-SiC or zinc-blende. The cubic SiC phase belongs to the space group Fd3m with crystalline structure of zincblende B3 bi-layer [12], that is face-centered cubic lattice with two atoms at the basis, with one

Si atom at the position 0, 0, 0 and the carbon atom at the position 1/4, 1/4, 1/4. This structure is considring in this work why because of all the preformances in SiC are more related.

1.4 Physical properties of silicon carbide (SiC)

The electronic properties of SiC differ for different polytypes. Almost all high temperature, high electric, and high frequency advantages of SiC devices are as the result of its wide band gap. The high electric field enables the device to with stand high breakdown voltage, as well. Therefore, the devices can be fabricated smaller for the same breakdown voltage, and the smaller the devices can be fabricated, the faster they can operate. In generally, Silicon Carbide Properties are Low density, High strength, Low thermal expansion, High thermal conductivity, High hardness, High elastic modulus, Excellent thermal shock resistance, Superior chemical inertness.

1.5 Application of silicon carbide (SiC)

There are many applications of silicon carbide, such as slide bearings, sealing rings, wear parts, sintering aids, heating elements, burner nozzles, heat exchangers [13].

1.6 Optical application of silicon carbide

Most of optical application of silicon-carbide are:[14]
. Materials engineered specifically for optical systems: in these case, Silicon carbide optical systems are engineered to exhibit low complexity, low mass, and a thermal designs, thereby providing enhanced system performance and reliability.
. Our SiC materials are ideally suited for mirrors and structural components for ground or space-based optical systems.
. CVD silicon carbide: is chemical vapor deposited, ultra high purity material used for mirrors or as an optical cladding for UltraSiC material.
. High-precision manufacturing: CoorsTek high-precision silicon carbide components feature wave front errors and surface roughness equal to or better than traditional substrates.

1.7 Conductivity of silicon carbide (SiC)

The high thermal conductivity allows high power density [13]. The high thermal conductivity makes SiC a better thermal conductor. Heat will flow more readily through SiC than Si material. This property enables SiC devices to operate at extremely high power levels and still dissipate the large amount of excess heat. Power losses are substantially reduced since SiC-based devices have high blocking voltage, and high operating temperatures as compared with silicon-based devices. SiC high-temperature devices, high-power, and high-frequency devices have wide

spectrum of applications from automotive engine sensors, jet engine ignition systems, transmitters for deep well drilling, to power supplies [5], and microwave transmitters [15, 16].

1.8 Silicon Carbide (SiC) Mobility

Among the different polytypes of SiC, the cubic phase shows a high electron mobility and the highest break-down field as well as saturation drift velocity [17, 18, 19]. Thus, the cubic phase is most effective for highly efficient high-performance electronic devices. A large number of traps become filled during the inversion causing the coulomb scattering of mobile charges and decreasing the mobility. The density of states (DOS) for the traps near the edge of the conduction band is so large, that they become comparable to the conduction band density of states (DOS) for electrons. This implies that a conduction band electron will have similar probabilities of occupying a conduction band trap or a conduction band state [20].

1.9 Electrical resistivity

Electrical resistivity, also known as volume resistivity, is the property which explains how difficult it is for electricity to pass through a material. Ceramics in general have high electrical resistivity. Therefore, they are commonly used as insulation materials. Some ceramics have electro conductive properties, such as SiC [21]. In this paper, we studied electron transport in silicon carbide system. We determined equilibirum lattice parameters, bulk modulus, k-points, cut-off energy and also calculated the energies, bandgap energies, bandsturctures, density of states (DOS) and projected density of state (PDOS), optical properties of silicon-carbide (SiC) and lastly workfunction of bulk SiC with in density functional theory and Monte Carlo transport simulator to supplement the result. The first-principles calculations were performed by using pseudopotential plane-waves approach and implemented in the ABINIT code and a GGA exchange-correlation within PBE is used.

1.10 Paper Organization

This paper is organized as follows. In chapter one, the introduction of SiC in general, physical property of SiC and application of SiC were considered. In chapter two, what we present DFT and MC methods as applied to study of electron transport in cubic SiC or zinc blende. In chapter 3, the result and discussion were presented and chapter 4 contains the conculsion part of the studies.

Chapter 2

Methods

2.1 Density Functional Theory(DFT)

2.1.1 Introduction

Density Functional Theory (DFT) is a computational quantum mechanical modeling method which can be used to investigate the structure and properties of atoms and molecules. Density functional theory allows investigators to make extremely complex many-body quantum mechanical system more tractable. Density functional theory is based on solving the Kohn-Sham equation for which a Noble Prize was awarded to Kohn in 1998. Since the roots of Kohn-Sham equation were formed on quantum mechanics. The story begins with the complexities of solving Schrödinger equation, which is the backbone of the quantum formulation. In case, Born-Oppenheimer approximation separates the mere nuclear from the electron parts. Although the electrons are still depends on the nuclear positions. Hartree manage the electron-electron correlation by reducing the many-electron wave function to single-electron ones. Hartree-Fock deals with the negligence of Hartree approximation by introducing the Slater determinant, which represents Pauli's exclusion principle [22]. Density functional theory is centered on the density of the electron instead of the wave function. Finally, Kohn-Sham formalism which is formally based on the electron density separates the parts of the electron-electron connection which can be calculated from those which cannot and ignore the latter part in the first step. Kohn-Sham genius idea in making approximations for their "ignorance" part which is called Exchange-Correlation, gained for Kohn the Noble Prize. The exchange-correlation was treated in the Generalized Gradient Approximation (GGA), as parameterized by Perdew, Burke, and Ernzehof (PBE). GGA using the Perdew-Burke-Ernzerh [23] at the Kohn-Sham DFT level. The DFT calculations are performed by using the ABINIT code [24] which is based on the plane-wave basis set.

2.1.2 Many-Body Schrödinger Equation

Quantum mechanics is a mathematical tool for predicting the behaviors of microscopic particles. The results of quantum formalism cover wide range of phenomena. In fact, one of the advantages of quantum mechanical calculations is its ability to

predict the total energy of a system of electrons and nuclei. Hence, electronic and geometric structure of solids can be predicted by total energy calculations and the relevant minimizations with respect to the electronic and nuclear coordinates. The properties of a non-relativistic, many-body quantum system are formulated in many-body Schrödinger equation. The simplest form of time-independent Schrödinger equation is

$$\hat{H}\Psi(r_1, \mathrm{r_2...r_n}, \mathrm{R_1}, \mathrm{R_2}.....\mathrm{R_m}) = E\Psi(r_1, \mathrm{r_2}, ...\mathrm{r_N}, \mathrm{R_1}, \mathrm{R_2}, ...\mathrm{R_M}) \tag{2.1}$$

The Hamiltonian of a system of electrons and nuclei is given by

$$\hat{H} = \hat{H}_\mathrm{e} + \hat{\mathrm{H}}_\mathrm{N} \tag{2.2}$$

Hamiltonian operator in ab-initio case.

$$\hat{H} = \frac{-\hbar^2}{2m_\mathrm{e}} \sum_\mathrm{i} \nabla_\mathrm{i}^2 + \sum_\mathrm{i,I} \frac{-\mathrm{Z_I e^2}}{|\overrightarrow{r_\mathrm{i}} - \overrightarrow{R_\mathrm{I}}|} + \frac{1}{2} \sum_\mathrm{i \neq j} \frac{\mathrm{e^2}}{|\overrightarrow{r_\mathrm{i}} - \overrightarrow{rj}|} - \sum_\mathrm{I} \frac{\hbar^2 \nabla_\mathrm{I}^2}{2\mathrm{M_I}} + \frac{1}{2} \sum_\mathrm{I \neq J} \frac{\mathrm{Z_I Z_J e^2}}{|\mathrm{R_I} - \mathrm{R_J}|} \tag{2.3}$$

The above Hamiltonian can be written in the following form:

$$\hat{H} = \hat{T}_\mathrm{e} + \hat{\mathrm{V}}_\mathrm{N-e} + \hat{\mathrm{V}}_\mathrm{e-e} + \hat{\mathrm{T}}_\mathrm{N} + \hat{\mathrm{V}}_\mathrm{N-N} \tag{2.4}$$

Where $\hbar$ the Plank constant, e is the electron charge, Z is the nuclei charge, m_e and M_I are mass of electron and nuclei respectively.
The first term is the electronic kinetic energy, the second term is electron-nuclei Coulomb attraction, the third term is the electron-electron repulsion, the fourth term is the nuclear kinetic energy and the last term is nuclei-nuclei repulsion.

2.1.3 Born Oppenheimer approximation

The electronic wave function depends upon the nuclear positions but not upon their velocities. The nuclear motion (such as rotation, vibration) feels the potential of fast-moving electrons[25]. The idea is to consider the wave functions of the couple system of nuclei and electrons as a combination of a complete set of states for electron at each nuclear position and the states of coupled electron-nuclear system; the latter ones are the functions of nuclear coordinates

$$\Psi(r_1, \mathrm{r_2}, ...\mathrm{r_N}, \mathrm{R_1}, \mathrm{R_2}, ..., \mathrm{R_M}) = \sum_\mathrm{i} \Psi(\mathrm{r_1}, \mathrm{r_2}, ...\mathrm{r_N}, \mathrm{R_1}, \mathrm{R_2}, ...\mathrm{R_M})\phi(\mathrm{R_1}, ...\mathrm{R_M})$$

$$\Psi(\{\overrightarrow{r}\}, \{\overrightarrow{R}\}) = \sum_i \Psi(\{\overrightarrow{r}\}, \{\overrightarrow{R}\})\phi(\{\overrightarrow{R}\}) \tag{2.5}$$

Where $\phi(R)$ is a nuclear wave function and $\Psi(\{r\}, \{R\})$ is electronic wave functions that depend parametrically on the nuclear positions.
Hamiltonian operator:

$$\hat{H} = \hat{H}_\mathrm{e} + \hat{H}_\mathrm{N} \tag{2.6}$$

Hamiltonian operator in electron:

$$\hat{H}_{\mathrm{e}} = \hat{T}_{\mathrm{e}} + \hat{\mathrm{U}}_{\mathrm{e-e}}(\{\overrightarrow{r}\}) + \hat{\mathrm{U}}_{\mathrm{e-N}}(\{\overrightarrow{r}\},(\{\overrightarrow{R}\}) \tag{2.7}$$

Hamiltonian operator in nuclear:

$$\hat{H}_{\mathrm{N}} = \hat{\mathrm{T}}_{\mathrm{N}} + \hat{\mathrm{U}}_{\mathrm{N-N}}(\{\overrightarrow{R}\}) \tag{2.8}$$

With Hamiltonian operator of electorn, wave function:

$$\hat{H}_{\mathrm{e}}\Psi(\{\overrightarrow{r}\},\{\overrightarrow{R}\}) = \hat{\mathrm{H}}_{\mathrm{e}}\phi(\{\overrightarrow{r}\},\{\overrightarrow{R}\}) \tag{2.9}$$

$$= E_{\mathrm{e}}\Phi(\{\overrightarrow{r}\};\{\overrightarrow{R}\}) \tag{2.10}$$

$$\hat{H}_{\mathrm{N}}\Psi(\{\overrightarrow{r}\};\{\overrightarrow{R}\}) = \hat{\mathrm{H}}_{\mathrm{N}}\phi(\{\overrightarrow{r}\};\{\overrightarrow{R}\}) \tag{2.11}$$

$$= E_{\mathrm{N}}\Phi(\{\overrightarrow{r}\};\{\overrightarrow{R}\}) \tag{2.12}$$

The total energy of the system is calculated by;

$$E = E_{\mathrm{e}} + \mathrm{E_N} \tag{2.13}$$

Where E_{e} total electronic energy and E_{N} total nuclear energy.
The force on the electron and nuclei are obtained according to:

$$F_{\mathrm{i}} = -\nabla_{\overrightarrow{r}_{\mathrm{i}}}\langle\Psi|\hat{\mathrm{H}}_{\mathrm{e}}|\Psi\rangle$$

$$= -\langle\Psi|\frac{\partial\hat{H}_{\mathrm{e}}}{\partial\overrightarrow{r}}|\Psi\rangle - \delta\frac{\langle\Psi|\hat{H}_{\mathrm{e}}|}{\delta|\Psi\rangle}\frac{\partial\langle\Psi|}{\partial\overrightarrow{r}_{\mathrm{i}}} \tag{2.14}$$

Upon geometry optimizations, the forces are minimized until effectively $F_{\mathrm{i}} \to 0$ and $F_{\mathrm{I}} \to 0$. When this happens, the ground state condition is said to be achieved and this corresponds to the state of the system with minimum energy. As an example, with the different approaches used in the different approximations of the interaction potentials, different convergence speeds and accuracies are seen.
That are Car-Parrinello Method (1985) states that [26]: Simultaneous solution of Kohn-Sham equations for electrons and Newton's equations for nuclei. Iterative update of wavefunctions, instead of diagonalization. Trace over occupied subspace to get total quantities (energy, forces, density) instead of eigenfunction calculations. Feasible due to simplicity of the plane wave pseudopotential method [27, 28].

2.1.4 Hohenberg-Kohn theorems

In 1964, Hohenberg and Kohn formulated and proved a theorem that established the density functional theory as a theory of many-body system. The theorem is proven for every system of non-interacting particles which has the Hamiltonian consisting of the electronic kinetic energy, external potential, and the electron-electron potential [29]
The theorem is divided into two parts:
Theorem I: The external potential is a unique functional of the electron density only. Thus the Hamiltonian, and hence all ground state properties, are determined

by the electron density as follows.
Hamiltonians opprators in Hohenberg-Kohn (HK):

$$\hat{H} = \hat{T} + \hat{V}_{\mathrm{ee}} + \hat{\mathrm{V}}_{\mathrm{ext}} \tag{2.15}$$

Above equation can be experssed as:

$$\hat{H} = \frac{\hbar^2}{2m}\sum_i \nabla_i^2 + \frac{1}{2}\sum_{i\neq j}\frac{e^2}{|r_{\mathrm{i}} - \mathrm{r_j}|} + \sum_i V_{\mathrm{ext}}(\mathrm{r_i}) \tag{2.16}$$

$$\hat{H}' = \hat{T} + \hat{V}_{\mathrm{ee}} + \hat{\mathrm{V}}'_{\mathrm{ext}} \tag{2.17}$$

These two potentials equations are the part of two different Hamiltonians which their only difference is in the external potential.
Theorem II: The ground state energy obtained variationally: the density that minimizes the total energy is the exact ground-state density. Then the ground state energy could be written as the functional of the ground state electron density:

$$E_0[\rho_0] = \mathrm{T}[\rho_0] + \mathrm{E_{ee}}[\rho_0] + \mathrm{E_{Ne}}[\rho_0] \tag{2.18}$$

where from equation 2.18,

$$T[\rho_0] + \mathrm{E_{ee}}[\rho_0] = \mathrm{F_{HF}} \tag{2.19}$$

Equation 2.19 is called the universal functional.
Hohenberg and Kohn approach follows from abstract formulation of expressing the Hamiltonian in eqn. (4), in terms of the electron density in 1964 by Hohenberg and Kohn [29]. That is,

$$\begin{aligned} H &= H[n(\overrightarrow{r})] \\ &= T[n(\overrightarrow{r})] + U_{\mathrm{e-e}}[\mathrm{n}(\overrightarrow{r})] + \mathrm{U_{e-N}}[\mathrm{n}(\overrightarrow{r})] + \mathrm{U_{N-N}}[\mathrm{n}(\overrightarrow{r})] \end{aligned} \tag{2.20}$$

$$N = \int (n(\overrightarrow{r})d\overrightarrow{r}) \tag{2.21}$$

where N is mean electron number;
$n(\overrightarrow{r})$ is mean electron density.

$$E = E[n(\overrightarrow{r})] = \frac{\langle\Psi|\hat{H}|\Psi\rangle}{\langle\Psi|\Psi\rangle} \equiv \frac{\langle\psi|\hat{H}|\psi\rangle}{\langle\psi|\psi\rangle} \tag{2.22}$$

Where E is the total energy of electron density.
According to the proposal, E can also be seen as

$$E[n(\overrightarrow{r})] = F[n(\overrightarrow{r})] + \int (U_{\mathrm{e-N}}(\{\overrightarrow{r}\};\{\overrightarrow{R}\})\mathrm{n}(\overrightarrow{r})\mathrm{d}\overrightarrow{r}) \tag{2.23}$$

$$F[n(\overrightarrow{r})] = T_{\mathrm{e}}[\mathrm{n}(\overrightarrow{r})] + \mathrm{U_{e-e}}[\mathrm{n}(\overrightarrow{r})] \tag{2.24}$$

Equation (24) is called universal function and has the same value regardless of the system as long as N remains same and

$$U_{\mathrm{e-N}}[\mathrm{n}(\overrightarrow{r})] = \int (\mathrm{U_{e-N}}(\{\overrightarrow{r}\};\{\overrightarrow{R}\})\mathrm{n}(\overrightarrow{r})\mathrm{d}\overrightarrow{r}) \tag{2.25}$$

2.1.5 Kohn-Sham equations

As a result, Walter Kohn and Luis Sham have proposed ways of explicitly expressing these functionals in terms of the electron density as follows [27, 29, 30]. Correspondingly, the Hamiltonian operator of a single electron is given as

$$\hat{H}_{\mathrm{ks}} = \frac{-\hbar^2\nabla_{\mathrm{i}}^2}{2\mathrm{m_i}} + \mathrm{V_{ks}}(\overrightarrow{r}, \mathrm{n}(\overrightarrow{r})) \tag{2.26}$$

with

$$\hat{H}_{\mathrm{ks}}\Psi_{\mathrm{i}}(\overrightarrow{r}) = \mathrm{E_i}\Psi_{\mathrm{i}}(\overrightarrow{r}) \tag{2.27}$$

where i =1,2,....N,

$$n(\overrightarrow{r}) = \sum_{i=1}^{N} |\Psi_{\mathrm{i}}(\overrightarrow{r})|^2 \tag{2.28}$$

$$E_{\mathrm{i}} = \langle\Psi_{\mathrm{i}}|\hat{\mathrm{H}}_{\mathrm{ks}}|\Psi_{\mathrm{i}}\rangle \tag{2.29}$$

where E_i is energy of the electron or is energy of the i^{th} electron.

$$E_{\mathrm{i}} = \mathrm{E_i}[\overrightarrow{r}, \mathrm{n}(\overrightarrow{r})] = \langle\Psi_{\mathrm{i}}\frac{|\hbar^2\nabla_{\mathrm{i}}^2|}{2\mathrm{m_i}}\Psi_{\mathrm{i}}\rangle + \langle\Psi_{\mathrm{i}}|\vee_{\mathrm{ks}}(\overrightarrow{r}, \mathrm{n}(\overrightarrow{r}))|\Psi_{\mathrm{i}}\rangle \tag{2.30}$$

$$\equiv T_{\mathrm{ks}} + \mathrm{U_{ks}}(\overrightarrow{r}, \mathrm{n}(\overrightarrow{r})) \tag{2.31}$$

The total electron energy for the system is

$$E_{\mathrm{e}} = \sum \mathrm{E_i}. \tag{2.32}$$

$$E_{\mathrm{e}} = \sum_{\mathrm{i=1}}^{\mathrm{N}}\langle\Psi_{\mathrm{i}}\frac{|-\hbar^2\nabla_{\mathrm{i}}^2|}{2\mathrm{m_i}}\Psi_{\mathrm{i}}\rangle + \sum_{\mathrm{i=1}}^{\mathrm{N}}\Psi_{\mathrm{i}}|\{\mathrm{V_{ks}}(\overrightarrow{r}, \mathrm{n}(\overrightarrow{r}))|\Psi_{\mathrm{i}}\rangle \tag{2.33}$$

$$\equiv T_{\mathrm{e}}[\mathrm{n}(\overrightarrow{r})] + \mathrm{U_{eff}}[\mathrm{n}(\overrightarrow{r})] \tag{2.34}$$

$$U_{\mathrm{eff}}[\mathrm{n}(\overrightarrow{r})] = \int \mathrm{V_{ks}}(\overrightarrow{r}, \mathrm{n}(\overrightarrow{r}))\mathrm{n}(\overrightarrow{r})\mathrm{d}\overrightarrow{r} \tag{2.35}$$

where U_{eff} is the effective potential energy with the Kohn-Sham model. Here

$$U_{\mathrm{eff}}[\mathrm{n}(\overrightarrow{r})] = \mathrm{U_H}[\mathrm{n}(\overrightarrow{r})] + \mathrm{U_{ext}}[\mathrm{n}(\overrightarrow{r})] + \mathrm{E_{xc}}[\mathrm{n}(\overrightarrow{r})] \tag{2.36}$$

where $U_{\mathrm{ext}}[\mathrm{n}(\overrightarrow{r})]$ -is the classical coulomb interaction potential energy between electrons, and
$U_{\mathrm{e-N}}[\mathrm{n}(\overrightarrow{r})]$ -is the interaction energy between electrons and nuclei,
which some times also may be represented as $U_{\mathrm{H}}[\mathrm{n}(\overrightarrow{r})]$.
E_{xc} -is the exchange correlation energy and is equal to the sum of the error made in using non-interacting kinetic energy and the error made in treating the electron-electron interaction classically (i.e arising due to quantum natures of electrons). With this the potenial is given as

$$V_{\mathrm{ks}} = \mathrm{V_{ks}}[(\overrightarrow{r}, \mathrm{n}(\overrightarrow{r}))] = \mathrm{V_H}[\overrightarrow{r}, \mathrm{n}(\overrightarrow{r})] + \mathrm{V_{xc}}[\overrightarrow{r}] + \mathrm{V_{e-N}}[\overrightarrow{r}] \tag{2.37}$$

Hamiltonian of an electron is

$$\hat{H}_{\mathrm{ks}} = \hat{\mathrm{T}}_{\mathrm{ks}} + \mathrm{V_{ks}} \tag{2.38}$$

From this, applying Schrödinger equation for the single electron, Corresponding Kohn-Sham equation

$$\hat{H}_{\mathrm{ks}}\Psi_{\mathrm{i}} = \mathrm{E_i}\Phi_{\mathrm{i}} \tag{2.39}$$

with

$$\varepsilon_{\mathrm{xc}} = \langle\Psi_{\mathrm{i}}|\mathrm{V_{xc}}|\Psi_{\mathrm{i}}\rangle \tag{2.40}$$

is being an exchange-correlation energy per electron, the total exchange-correlation energy for all electrons, E_{xc}, can be given as:

$$E_{\mathrm{xc}} = \mathrm{E_{xc}}[\mathrm{n}(\overrightarrow{r})] = \int \mathrm{V_{xc}}[\overrightarrow{r}, \mathrm{n}(\overrightarrow{r})]\mathrm{n}(\overrightarrow{r})\mathrm{d}\overrightarrow{r} \tag{2.41}$$

Correspondingly also, Total Hatree potential

$$U_{\mathrm{H}} = \mathrm{U_H}[\mathrm{n}(\overrightarrow{r})] = \int \mathrm{V_H}[\overrightarrow{r}, \mathrm{n}(\overrightarrow{r})]\mathrm{n}(\overrightarrow{r})\mathrm{d}\overrightarrow{r} \tag{2.42}$$

and total electron-nuclei interaction energy,

$$U_{\mathrm{e-N}} = \mathrm{U_{e-N}}[\mathrm{n}(\overrightarrow{r})] = \int \mathrm{V_{e-N}}[\overrightarrow{r}]\mathrm{n}(\overrightarrow{r})\mathrm{d}\overrightarrow{r} \tag{2.43}$$

where U_{H} and $U_{\mathrm{e-N}}$ are the classical coulomb potential energy (Hatree potential energy) and the total potential energy of interaction between electrons and nuclei, respectively. The total electron-electron interaction potential energy $U_{\mathrm{e-e}}$ is thus seen as:

$$U_{\mathrm{e-e}} = \mathrm{U_{e-e}}[\mathrm{n}(\overrightarrow{r})] = \mathrm{U_H}[\mathrm{n}(\overrightarrow{r})] + \mathrm{E_{xc}}[\mathrm{n}(\overrightarrow{r})] \tag{2.44}$$

The total energy E of the system of N electrons and M nuclei is thus given as the sum of the electronic term and nuclear term,
i.e $E = E_{\mathrm{e}} + \mathrm{E_N}$.
The force on each electron is given according to:

$$\begin{aligned} F_{\mathrm{i}} &= -\nabla_{\overrightarrow{r}}\langle\Psi_{\mathrm{i}}|\hat{\mathrm{H}}|\Psi_{\mathrm{i}}\rangle = -\langle\Psi_{\mathrm{i}}|\nabla_{\overrightarrow{r}}\mathrm{V_{ks}}|\Psi_{\mathrm{i}}\rangle \\ &\equiv -\langle\Psi_{\mathrm{i}}|\frac{\partial\hat{\mathrm{H}}_{\mathrm{ks}}|}{\partial\mathrm{r}}\Psi_{\mathrm{i}}\rangle - \delta\langle\Psi_{\mathrm{i}}|\frac{\hat{\mathrm{H}}_{\mathrm{ks}}|}{\delta|\Psi_{\mathrm{i}}\rangle}\Psi_{\mathrm{i}}\rangle\frac{\partial\langle\Psi_{\mathrm{i}}|}{\partial\mathrm{r}} \end{aligned} \tag{2.45}$$

2.1.6 Exchange-correlation energy

Beginning with the Thomas-Fermi model [30, 31] to describe the form of electron density for a uniform electron gas (i. e. assumed as homogeneous and non-interacting), the first approximation for these quantities is made and practically implemented in 1965 by W. Kohn and L. Sham [30]. Ever since, this approach of estimating has been known, updated, and used as **Local density approximation (LDA)** in many density functional theory codes. The concept of uniform electron gas is at the center of LDA. The uniform electron gas refers to electrons moving in a positive charge distribution in a way that the system is electrically neutral. Although LDA is based on a not realistic assumption of uniform electron gas, its exchange-correlation functional is exactly calculated and this is the reason

of its importance. The exchange-correlation of Kohn-Sham equation is defined as the exchange potential for the spatially uniform electron gas with the same density as the local electron density.

Generalized Gradient Approximation (GGA): the exchange-correlation energy does not include the non-local contributions resulted from the in-homogeneities in the real electron density at a distance from the element.

$$E_{\mathrm{xc}}^{GGA} = \int \mathrm{d}_{\mathrm{r}}^{3} \epsilon_{\mathrm{xc}}^{\mathrm{GGA}}(\mathrm{n(r)}, \nabla \mathrm{n(r)}) \tag{2.46}$$

Total exchange-correlation energy

$$E_{\mathrm{xc}} = \mathrm{E_{xc}}[\mathrm{n}(\overrightarrow{r}] = \int \mathrm{V_{xc}}(\overrightarrow{r})\mathrm{n}(\overrightarrow{r})\mathrm{d}\overrightarrow{r} \tag{2.47}$$

and also, in an other exepression,

$$E_{\mathrm{xc}} = \int \varepsilon_{\mathrm{xc}} \mathrm{f}[\rho, \nabla\rho]\rho(\mathrm{r})\mathrm{d}^{3}\mathrm{r} \tag{2.48}$$

This equation depends only on the general feature of the real space construction where (f) is a parameterized analytic function, and (∇) is the gradient density of the electrons. The equation above is only based on the systems of non-spin electrons. If we consider the system containing electrons with different spins, the system exhibits magnetism and is a straightforward spin polarized material. Now the equation above will take the form of spin densities,

$$E_{\mathrm{xc}}[\rho\uparrow, \rho\downarrow] = \int \varepsilon_{\mathrm{xc}} \mathrm{f}[\rho\uparrow, \rho\downarrow, \nabla\rho\uparrow, \nabla\rho\downarrow]\rho(\mathrm{r})\mathrm{d}^{3}\mathrm{r} \tag{2.49}$$

2.1.7 Pseudopotentials

The pseudopotential plane wave is one of the most common methods used for calculating the external potential of Kohn-Sham equation. The electron-nuclei interaction term is set to be approximated. Since the potential energy for the electrons in the vicinity of the nucleus diverges, the wave-functions fluctuate rapidly. So, smoothing effect required. The advantage of using pseudopotential is approximate the properties of core electrons in a way that could reduce the number of plane waves in a calculation. In what is called Pseudopotential usage for the core electrons [29] -[33]. Therefore; Pseudopotential have three significant motivations behind the pseudopotential philosophy [34]

(1) it reduces the basic set size in the calculation,

(2) it decreases the number of electrons; and

(3) allows the possibility of including the relativistic effects in the whole estimation. The real and pseudo wave function and potentials match above a certain radius r_{c}. where ψ_{pseudo} is pseudowavefunction; ψ_{AE} is all-electron wave function; V_{pseudo} is pseudopotetials; $\frac{z}{r}$ is all electron potential and r_{c} is cutoff radus.

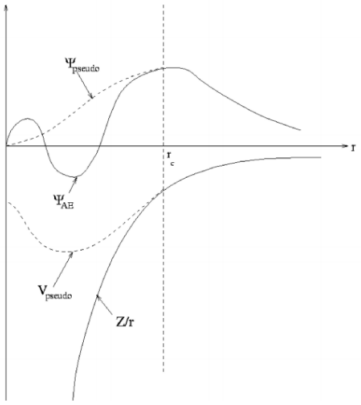

Figure 2.1: Comparison of a wave function in the potential of the nucleus to the one in the pseudopotential.

2.1.8 Equlibrium lattice constant(a_0) and bulk modulus (B_0) of SiC.

The total energy of a system varies with structure in a cubic crystal with a single lattice parameter. i.e Changing the lattice parameter, changes the volume of the unit cell, and the volume that minimizes the total energy gives the equilibrium volume. The bulk modulus is closely related to the E(V) and it is proportional to the curvature of the equation of state at the equilibrium volume:[35]-[37].
The third-order Birch-Murnaghan isothermal equation of state (eos) is given by

$$P(V) = \frac{3B_0}{2}[(\frac{V_0}{V})^{\frac{7}{3}} - (\frac{V_0}{V})^{\frac{5}{3}}]\{1 + \frac{3}{4}(B_0' - 4)[(\frac{\mathrm{V_0}}{\mathrm{V}})^{\frac{2}{3}} - 1]\}. \tag{2.50}$$

The bulk modulus and its derivative are usually obtained from fits to experimental data and are defined as:

$$B_0 = -\mathrm{V}\frac{\partial \mathrm{P}}{\partial \mathrm{V}}|_{\mathrm{V=V_0}} = \mathrm{V}\frac{\partial^2 \mathrm{E}}{\partial \mathrm{V}^2}|_{\mathrm{V=V_0}} \tag{2.51}$$

where B_0- is the bulk modulus.It is anumerically sensetive quantity.
V- is the volume particles;
V_o- is initial or groud state volume ;
P- is the pressure of particles; and
$E(V)$ - is the energy of the particles with respect to volume function.
In an other way the derivative of the bulk modulus with respect to pressure, evaluated at the equilibrium volume:

$$B1 = (\frac{\partial B}{\partial V})|_{V=V_0} \tag{2.52}$$

$$= \frac{\partial}{\partial P}(V\frac{\partial^2 E}{\partial V^2})|_{\mathrm{V=V_0}} \tag{2.53}$$

where $B1$ is the derivative of the bulk modulus.
It is a third-order derivative of the energy(E) and hence describes effects that are one order higher even than the bulk modulus. It is related to the volume-dependence of the $E(V)$ curvature. $B1$ is therefore the most sensitive elastic quantity. The results can then be compared to experiments and allowing the accuracy

of the planewave pseudopotential method to be determined calculations. In this work we use Birch-Murnaghan equation of state method of fitting to determine the equlibrium lattice parameter of the SiC.

2.1.9 K-point sampling (kpts optimum).

In reciprocal space, the phases are nodes or points in the unit cell, which are described by sampling the Brillouin zone (BZ). The BZ describes the unique region of space closest to the $\mathbf{G} = \mathbf{0}$ point onto which all other points can be mapped by periodicity, therefore by sampling the BZ, the entirety of the bulk is sampled. The change in energy when sampling k-points determines how many of them need to be sampled, that is, an energy convergence test (or other property of interest) is carried out using an increasing number of k-points. The need for k-points arises directly from Bloch's theorem, which states that in a periodic potential the wavefunctions have a periodic magnitude, but it says nothing about their phase (since wavefunctions are complex they possess both a magnitude and a phase). Bloch's theorem which state that [38]

$$\psi_{\mathrm{k}}(\mathrm{r}) = \sum_{\mathrm{G}} \mathrm{C_k}, \mathrm{G}^{\mathrm{i(G+k).r}} \tag{2.54}$$

A uniform mesh of $k-$points, valid for any crystal, generated by Monkhorst-Pack procedure has the following form:

$$\overrightarrow{K}_{\mathrm{n1,n2,n3}} = \sum_{1}^{3} \frac{2\mathrm{n_i} - \mathrm{N_i} - 1}{2\mathrm{N_i}} \overrightarrow{G}_{\mathrm{i}} \tag{2.55}$$

where N_{i} is the number of $k-$points in each direction and n_{i} =1,..., N_i and G_i is the primitive vectors of the reciprocal lattice [39].

2.1.10 Plane wave cut-off energy (ecut optimum).

In this we have done by means of a convergence test (systematic convergence with single parameter), in which we perform a series of calculations, using increasing cut-off energy, and keeping the convergerice of the total energy towards its large cut-off limit. For these purposes, we only need to use single k-point to sample the Brillouin zone. This is because we are only seeking to determine a suitable cut-off energy for convergence rather than a final result. However, we choose to give the k-point of 400 eV as this is known to give a more accurate answer at no extra computational expense. Practical implementations require a complete specification of the single particle Bloch states, whose periodic part $C_{i,k}$ can be expressed as [37, 38].

$$C_{\mathrm{i,k}}(\mathrm{r}) = \frac{1}{\sqrt{\mathrm{V_{cell}}}} \sum_{\mathrm{G}} \mathrm{C_{i.k}} + \mathrm{Ge}^{\mathrm{iG.r}} \tag{2.56}$$

where

$$\sum_{G} |C_{\mathrm{i,k+G}}|^2 = 1 \tag{2.57}$$

and G are reciprocal lattice vectors. Evaluating the kinetic energy part of the eigenstate (i, k) gives

$$T = \sum_{\mathrm{G}}^{G_{max}} |\mathrm{C_{i,k}} + \mathrm{G}|^2 \frac{\hbar^2}{2\mathrm{m}} (\mathrm{K} + \mathrm{G})^2 \tag{2.58}$$

Now, with the possibility of an infinite number of G vectors, such calculations for all eigenstates (i, k) are not feasible. A common practice is thus to truncate the G value to some $G_{\mathrm{max}} < \mathrm{G_{cut}} - \mathrm{k}$

$$C_{\mathrm{i,k}}\mathrm{r} = \frac{1}{\sqrt{\mathrm{V_{cell}}}} \sum_{\mathrm{G}}^{\mathrm{G_{max}}} \mathrm{C_{i,k}} + \mathrm{Ge^{iG.r}} \tag{2.59}$$

From equation above (2.58), it can be seen that the kinetic energy T is less than that of the cutoff energy E_{cut} , that is:

$$E_{cut} = \frac{\hbar^2}{2m} G_{\mathrm{cut}}^2 \tag{2.60}$$

2.1.11 Surface energy

The surface energy is related to the work needed to split an infinite crystal in two semi-infinite crystals. It has a direct relation with the number and strength of the bonds which are broken to create the surface and consequently, surface energies for different facets of the same solid can differ [40, 41].
Mathematically it can be callculeted as

$$\sigma = \frac{1}{2A}[E_{\mathrm{slab}} - \frac{\mathrm{N_{slab}}}{\mathrm{N_{bulk}}} \times \mathrm{E_{bulk}}] \tag{2.61}$$

where N_{slab} - means Number of atoms per unit cell of the slab, and , N_{bulk} - means number of atoms per unit cell of the bulk, while , E_{slab} and E_{bulk} - mean total energy of the slab, and bulk unit cell, respectively and A is the specific surface area of the employed slab model.

2.1.12 Cohesive energy

Cohesive energy is the energy that must be supplied to the solid to separate its constituents into neutral free atoms at rest and at infinite separation with the same electronic configuration.
The cohesive energy is also an important physical quantity that accounts for the bond strength of a solid, which equals the energy needed to divide the solid into isolated atoms by breaking all the bonds.
Cohesive energy is also a basic quantity for thermodynamics, by which almost all thermodynamic properties of materials can derive. Consider the unit cell of N atoms; the bulk cohesive energy $E_{\mathrm{coh}}(\infty)$ per unit cell is [40, 42];

$$Ecoh = \frac{1}{N[E_{\mathrm{tot}}(\infty) - \sum_{\mathrm{N}} \mathrm{E_{iso}}]}$$

where
E_{iso} is the energy of an isolated atoms, E_{coh} bulk cohesive energy, $E_{\mathrm{tot}}(\infty)$ is bulk cohesive energy per unit cell
And also other expersion of cohesive energy as bulk are follows:

$$E_{\mathrm{coh}} = \frac{1}{\mathrm{N}}[\mathrm{SE_{atom}} - \mathrm{E_{bulk}}]$$

where
N is number of atom in unit cell, E_{bulk} is the total energy of bulk, E_{atom} is the total energy of atom,

2.1.13 Work Function

The work function gives a measure of how tightly a particular materials holds the electrons. Because any variation in the surface ionic and electronic charge distribution gives changes in the work function, so it does any change in the orientation, relaxations, reconstructions and absorbed molecules. Consequently the work function is very important in the characterization of surfaces [43].
The Fermi energy, E_{f} refers to the energy of the highest occupied electronic state of the system. At ground level or 0 K and a perfect vacuum, the workfunction is the energy difference betweenn the Fermi level and the vacuum level, which can be written as

$$\Phi = \Phi_{\mathrm{v}} - \Phi_{\mathrm{f}} \tag{2.62}$$

where Φ is workfunction, Φ_v is vacuum energy, and Φ_f is fermi energy.
For a symmetric surface, the vacuum level E_v is defined as the converged electrostatic poetential outside the slab surface. Due to the periodic condition, the vacuum potential is taken as the halfway point of the vacuum slab above the surface where the influence from the adjacent cell is minimum.
The adsorption energy of the reaction intermediates on the SiC surfaces is defined as

$$E_{\mathrm{ads}} = \frac{\mathrm{E_{ads+slab}} - \mathrm{N.E_{ads}} - \mathrm{E_{slab}}}{\mathrm{N}} \tag{2.63}$$

where E_{ads} - is the total energy of the adsorbates, $E_{ads+slab}$ - is the total energy of the adsorbate with the SiC surface slabs, E_{slab} - is the total energy of the corresponding contaminant free slabs, N - is the number of molecules on the surface.
The work function (in volts) of the metal, ϕ_{M}, and the semiconductor, ϕ_{s} - is the energy required to remove an electron from the respective Fermi levels to vacuum. Mathmatically it defined as:

$$\phi_{\mathrm{s}} = \mathrm{X_s} + \mathrm{V_N} \tag{2.64}$$

where X_{s} is the electron affinity, and V_{N} is the energy difference, between the conduction band and the Fermi level of the semiconductor relate to the work function. where

$$V_{\mathrm{N}} = \frac{\mathrm{KT}}{\mathrm{q}} \ln(\frac{\mathrm{N_C}}{\mathrm{n_e}}) \tag{2.65}$$

where n_e is the density of electrons in the conduction band.

2.1.14 Computational Implementation

ABINIT: It is a software that allows one to perform first-principles calculations in the framework of:
. Density-Functional Theory (DFT) → ground-state
. Many-Body Perturbation Theory (MBPT) → excited-states
. Density-Functional Perturbation Theory (DFPT):- in response to atomic displacements, to static homogeneous electric field, and to strain perturbations.
. In Second-order derivatives of the energy, giving direct access to: dynamical matrices at any q, phonon frequencies, force constants; phonon DOS, thermodynamic properties (quasi-harmonic approximation); dielectric tensor, Born effective charges; elastic constants, internalstrain; piezoelectric tensor.
ABINIT is capable in:
. Basis sets like, planewaves, projector augmented waves (PAW) and wavelets (BIGDFT effort),
. Representation of atoms in: different PAW generators, many norm-conserving pseudopotential types,
. Exchange-correlation functionals for DFT in: GGA, LDA, LDA+U (only with PAW), + some advanced functionals (Meta-GGA, RPA) [24].
Abinit emphasizes on computing:- lattice constant, bulk modules and equilibrium energies of solids. It also includes option to optimize the geometry according to the DFT forces and stresses. Excited states can be computed within the many body- body perturbation theory.

2.1.15 Optical property of SiC

With its character of wide band-gap, high breakdown critical field strength, high electron mobility and strong ability to resist radiation and so on, SiC has a broad prospect of application [44, 45]. The optical properties of semiconductor and its basic optical function play an important role in the application of materials and devices of semiconductor. The electron wave function is expanded in plane waves up to a cutoff energy of 400 eV.

Dielectric function

In measuring optical properties, the frequency-dependent imaginary part of the dielectric function $\varepsilon^{(2)}_{\alpha\beta}(\omega)$ was determined by the summation of empty states according to the following equation:

$$\varepsilon^{(2)}_{\alpha\beta}(\omega) = \frac{4\pi^2 e^2}{\Omega}\frac{1}{q^2}\lim_{q\to 0}\sum_{c,\nu,k} 2\omega_k \delta(e_{ck} - e_{\nu,k} - \omega) \times \langle u_{ck} + e_a u\rangle^* \tag{2.66}$$

where c and v refer to the conduction and valence band states, respectively, and u_{ck} is the cell periodic part of the wave functions at k-point k.

The real and imaginary parts of the analytical dielectric function are connected by the Kramers-Kronig relation as[45]

$$\varepsilon^{(1)}_{\alpha\beta}(\omega) = 1 + \frac{2p}{\Pi}\int_0^\infty \frac{\varepsilon^2_\alpha \beta(\omega')\omega'}{\omega'^2 - \omega^2 + \mathrm{i}\eta}\mathrm{d}\omega' \tag{2.67}$$

where P denotes the principal value.
The refractive index and absorption coefficient are defined as:

$$n = [(\frac{\sqrt{\varepsilon_1^2 + \varepsilon_2^2} + \varepsilon_1}{2})]^{\frac{1}{2}} \tag{2.68}$$

$$\alpha = [2(\sqrt{\varepsilon_1^2 + \varepsilon_2^2} + \varepsilon_\varepsilon)]^{\frac{1}{2}} \tag{2.69}$$

where n is refractive index ε_1, ε_2 are dielectric constants and α absorption coefficents.

Absorption

It is linearly related to the imaginary part of the macroscopic dielectric constant (frequency dependant).
i.e

$$E(x,t) = E_0 \mathrm{e}^{\frac{\mathrm{i}\omega}{\mathrm{c}}\times\tilde{\mathrm{n}}}\mathrm{e}^{-\mathrm{i}\omega\mathrm{t}} \tag{2.70}$$

$$\tilde{n} = \sqrt{\epsilon} = n + ik \tag{2.71}$$

$$\epsilon = \epsilon_1 + \mathrm{i}\epsilon \tag{2.72}$$

Electron energy loss spectrocopy (EELS)

Electron energy loss spectroscopy (EELS) is the technique to measure the amount of energy loss in an inelastic scattering event, when electrons pass through the material [46]. Transmission electron microscopy (TEM) is the appropriate microscope for EELS since in order to have the projection image, electrons should transport in the material [47]. EELS has been successfully used for the measurement of electronic structure [48], optical properties, density and thickness of thin film specimens.
Electron energy loss spectra (EELS) can be used to explore the plasmonic (collective electronic) excitations of an extended system. This is because the energy loss of a fast electron passing by a material is defined by:

$$EELS = Im\frac{1}{\varepsilon(q,\omega)} \tag{2.73}$$

and the plasmon frequency ω_p is defined as when $\varepsilon(\omega) \to 0$. It means that an external perturbation at this frequency, even infinitesimal, can generate large collective electronic response.

2.1.16 Electron transport simulation of SiC using DFT calculated density of state (DOS)

The Monte Carlo method [49] takes into account scattering events and band structure model to investigate electron transport. Then the macroscopic mobility is obtained from averaging the drift velocity with respect to external electric field. The simplest approach, as described in [50] takes into account analytical formulas for energy band structure and density of states(DOS). This approach is correct only for very low energies and ideal crystalline structures. In [51, 52] it was proposed to use simple equations of scattering rates and combine these formulas with numerically calculated by the means of DFT method DOS. The density of states (DOS) of a system describes the number of states that could be occupied at each energy level. A high DOS at a specific energy level means that there are many states available for occupation. The density of states can be calculated from band theory calculations. It is calculated either as a function of energy E or the wave vector k [53]. The contribution of the eigenstate at $E = E_{\mathrm{k}}$ to the total density of states is $\delta(E - E_{\mathrm{k}})$ and therefore DOS(E) can be expressed as:

$$DOS(E) = \sum_{allEk} \delta(E - E_k) \tag{2.74}$$

The local density of states $d_{\mathrm{n}}(\mathrm{E})$ associated with the basis state $|n\rangle$ at energy E is calculated by considering the weight factor for each energy contribution:

$$d_n(E) = \sum_{allE_{\mathrm{k}}} |\langle n|\Psi_{\mathrm{k}}\rangle|^2 \delta(E - E_{\mathrm{k}}) \tag{2.75}$$

In general, the total density of states is recovered by summing all local densities of states:

$$DOS(E) = \sum_{alnl} d_{\mathrm{n}}(\mathrm{E}) = \sum_{\mathrm{allE_k}} \delta(\mathrm{E} - \mathrm{E_k}) \tag{2.76}$$

The normalization condition of the eigenstate is:

$$\sum_{allE_{\mathrm{k}}} |\langle n|\Psi_{\mathrm{k}}\rangle|^2 = 1. \tag{2.77}$$

where $d_{\mathrm{n}}(\mathrm{E})$ is the local density of states.

2.1.17 Electron transport simulation of SiC using DFT calculated projected density of state (PDOS)

The projected density of states is the density of states due to small group of atoms in the material. The projected density of states provides the contributions of each atomic orbital in the structure. Therefore, the equation of PDOS over i gives the spectral weight of orbital i, is:

$$\rho_i(E) = \sum_n \langle \Psi_{\mathrm{n}}|\mathrm{i}\rangle\langle \mathrm{i}|\Psi_{\mathrm{n}}\rangle \delta(\mathrm{E} - \mathrm{E_n}) \tag{2.78}$$

where $\sum_i |i\rangle\langle i| = 1$, this is orthonormal basis,
E_{n} is the eigenvalue and $|\Psi_{\mathrm{n}}\rangle$, is the eigenstate.

2.1.18 Bandgap energy

The bandgaps are retrieved in the band structure is calculated by DFT-GGA (PBE) [51]. The band gap of silicon carbide in this work is almost 2.448 eV. Based on the band structures, materials have either direct band gap or indirect band gap. If the momentum of the lowest energy state in the conduction band and the highest energy state of the valence band of a material are the same, the material has a direct bandgap. If they are not the same, then the material has an indirect band gap. For materials with a direct band gap, valence electrons can be directly excited into the conduction band by a photon whose energy is larger than the bandgap. In contrast, for materials with an indirect band gap, a photon and phonon must both be involved in a transition from the valence band top to the conduction band bottom. Therefore, direct bandgap materials tend to have stronger light emission and absorption properties. Other things equal, direct bandgap materials tend to be better for photovoltaics (PVs), light-emitting diodes (LEDs), and laser diodes; however, indirect bandgap materials are frequently used in PVs and LEDs when the materials have other favorable properties [54].
The band structure of semiconductors are the energies of one-particle excitations, which is related to the difference between total energies of states differing by one electron. In particular, the lowest conduction-band energy is given by:

$$E_{\mathrm{c}} = \mathrm{E_{N+1}} + \mathrm{E_N} \tag{2.79}$$

where $E_{\mathrm{N+1}}$ is the negative of the electron affinity of the N-particle system and E_{N} is the negative of the first ionization energy of the same N-particle system.
The highest valence-band energy is given by:

$$E_{\mathrm{V}} = \mathrm{E_N} - \mathrm{E_{N-1}} \tag{2.80}$$

The bandgap energy E_{G} is the energy defined as the difference between the conduction band E_{C} and the valence band E_{V}

$$E_{\mathrm{G}} = \mathrm{E_C} - \mathrm{E_V}. \tag{2.81}$$

2.2 Monte Carlo Methods

2.2.1 Introduction

The strength of the Monte Carlo method is the ability to accurately simulate physical phenomena using a very detailed computer simulation model. The Monte Carlo Mthodes essentially solves the Boltzmann transport equation through a computer simulation of the dynamics of carrier transport. It relies on a semiclassical approach. The Boltzmann transport equation model has been the main tool used in the analysis of transport in semiconductors. Free carriers are treated as classical point-like particles, which in the absence of scattering, drift in an external field $\overrightarrow{F}$ according to Newton's equation of motion [55].

$$e\overrightarrow{F} = \hbar\frac{d\overrightarrow{k}}{dt} \tag{2.82}$$

where $e\overrightarrow{F}$ is external fieled, $\frac{d\overrightarrow{k}}{dt}$ is drift velocity.
For this approximation to be used, the length scale in the direction of $\overrightarrow{F}$ must be much larger than the size of the semiconductor unit cell in that direction. If this is true, then the carrier energy spectrum is approximately continuous in the electron wavevector, $\overrightarrow{k}$, and carriers can be described as point-like wavepackets.
At the beginning of the Monte Carlo simulations of **electron transport**, the simulated electron is placed at the conduction band minimum. The steady-state results are however independent of the choice of initial state. The electron is then allowed to drift in the applied field according to equation (2.74), for a specified drift time T_{d}. This drift time is chosen so that it is always much smaller than the inverse of the scattering rate. After the drift, it is determined whether a scattering event will occur. The simulation continues through a series of drifts and scattering events, until the convergence of the average electron velocity along the direction of the driving field.

$$\vartheta_{\mathrm{d}} = \frac{\mathrm{p_{sc}}}{\mathrm{eF}} \tag{2.83}$$

This equation is useful to determine the convergence of the MCM simulations. When the drift velocity is accurately obtained, the results are similar [55].
The Monte Carlo simulator was then used to calculate the electron scattering rates, average velocity, and mobility. In general, the Monte Carlo method is a semi-classical technique, which simulates electrons as classical particles undergoing scattering events separated by drifts in an electric field.

Chapter 3

Results and Discussion

In this chapter a brife discussion had been taken. we discussed the determination of equilibrium lattice constant, bulk modulus, convergence of cut-off energy, convergence of K-points samppling in BZ. And also we have discussed different energies and correlating with other exprimental works as well as, we have performed bandstructure, DOS, PDOS, Optical properties, and workfunction with GGA and PBE correlation combined with the results from other experimental data.

3.1 Determination of equlibrium lattice constant (a_o) of SiC

The cubic SiC phase belongs to the space group Fd3m with crystalline structure of zincblend B3 bilayer, that is face-centered cubic lattice with two atoms at the basis, with one Si atom at the position 0, 0, 0 and the carbon atom at the position 1/4, 1/4, 1/4. We have obtained through a total energy minimization process a lattice constant value of the cubic phase $a_0 = 4.38$Å, slightly smaller than that of calculated by $a_0 = 4.39$Å, [56] using the pseudopotential method PBE.

Table 3.1: Equlibrium lattice parameter and Bulk modulus for: bulk carbon (C), bulk silicon (Si) and, bulk SiC [56]

parameters	C	Si	SiC
a_o in(Å)	3.54	5.45	4.38
refefernce[56, 57]	3.56	5.44	4.39 ,4.38
B_0(in Gpa)	454.301	110.202	201.36
refefernce[58]	406.77	90.817	202

Therefore, the equlibrium lattice constant value calculated for SiC bulk structures are in excellent agreement for PBE (4.38 Å) compered to reported exeprimental data shown in table 3.1 [56] (4.39Å) and exactly equal value of exprimental result with [57] (4.38Å). And by using the total energy curves vs cell volume curve of SiC as shown in the figure 3.1. The minimum point on the curve corresponds to the equilibrium volume of the unit cell which gives us the equilibrium lattice constant.

3.2 Determination of Bulk Modulus (B_0)

The exprimental vulue of bulk modulus for SiC simulation in abinit code was 202Gpa. The calculated value for SiC by using the same code was 201.36 Gpa. Based on the information listed in table 3.1, the bulk modulus obtained from PBE, is very closely agree value with comparision to the exprimental one (202 Gpa) [57]. The graph of bulk carbon zincblende, silicon zincblend and bulk silicon carbide value from total energy vs volume, shown as follows.

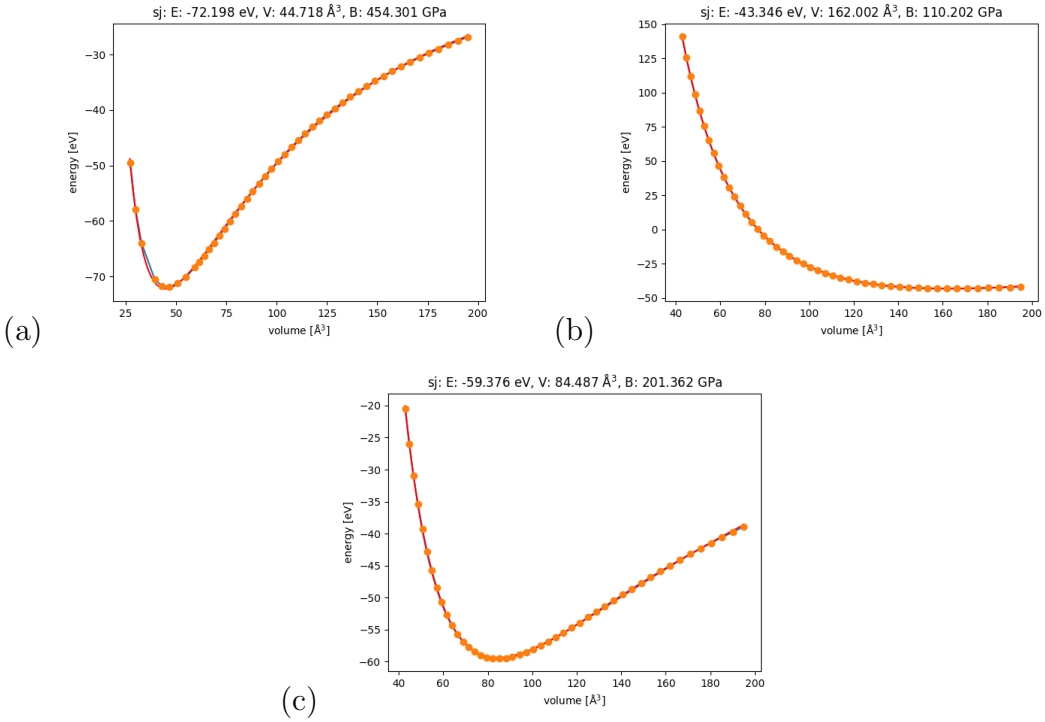

Figure 3.1: Convergence of lattice constant, bulk modulus, from the total energy vs volume for (a), bulk carbon zincblende, (b), bulk silicon zincblende and (c), bulk silicon carbide zincblende eos respectively.

3.3 The convergence of the K-point sampling

K-point convergence of SiC was analysed in the unit cell by varying the Monkhorst-Pack gird the calculeted value for SiC in PBE yileds by using simulation in abinit code is 4x4x4. The graph of total energy against kpts for SiC as follow:

3.4 Plane wave Cut-off energy (ecut optimum)

To obtain reliable results, the cutoff energy values should be selected carefully, and experience shows that values of 350-450 eV [57] are often satisfactory for most systems. Thus in our system the calculated value for SiC by simulation in abinit code with PBE, the cut off energy of the plane wave is set to be 400 eV. This

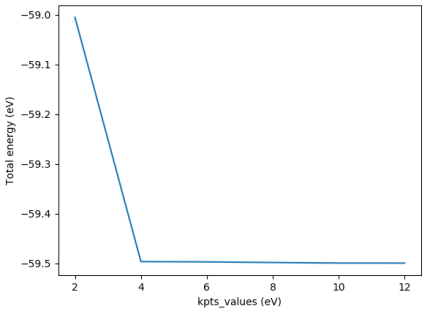

Figure 3.2: Total energy convergence of SiC as a function of K-points.

shows that our systems is very good agreed estimation reliable results. Because it found between the satisfactory interival 350-450eV. The graph of total energy vs ecut is shwon as follow.

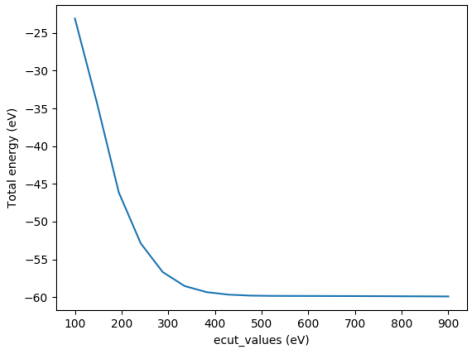

Figure 3.3: Convergence of the total energy of cubic SiC as a function of planewave cut-off energy [54].

3.5 Exechange-Correlation potential (xc optimum)

The exchange-correlation potential is the functional derivative of the exchange-correlation energy; however, there is no universal form for exchange-correlation functionals and there are several methods suggesting the exchange-correlation functional approximation [58]. Such as local density approximation (LDA) which is uniform electron gas (in the homogeneous electron gas) with this density by different scientist(Kohon-Sham), Monte Carlo and the genral gradint approximation (GGA) which is none uniform electron gas(hetrogeneous electron gas) with this density. The exchange-correlation in this system through out the work is PBE or GGA, not LDA.

3.6 Psedopotentials optimum (pps)

Pseudopotentials are a Materials Relation providing an approximation of the full Hamiltonian. They can be developed to approximate the core (i.e non-valence) electrons of an atom and its nucleus with an effective potential, or pseudopotential. This approach considers the nuclear charge as effectively screened by tightly bound core electrons. This has two consequences: only the chemically active valence electrons are treated explicitly, and the potential profile they experience is much smoother, there by reducing the number of electrons in the Schrödinger equation and the size of basis sets [32]. For all the calculations done in this work, we used the FHI pseudopotentials developed at the Fritz-Haber-Institute. The FHI was used to perform the total energy calculations within the pseudopotential framework for all systems here considered [34], [37].

3.7 Detremination of Surface geometries optimization of SiC energy, cohesive energy and vacancy energy of SiC.

We first determined the cell parameter of our cubic zinc-blende, SiC structure since the surface slab is generated from the bulk material. Our optimized parameters are carbon, Silicon and cubic-SiC or zinc-blende and the result is in good agreement with experimental results and other first principles quantum mechanical calculations. Acording to the result listed in table 3.2, SiC (100), SiC (110) and SiC (111) surface was geometry optimized giving a calculated surface energy of 0.3169655 $eV/\mathring{A}^2$, 0.2277070 $eV/\mathring{A}^2$ and 0.43674081$eV/\mathring{A}^2$ respectively and compared these result with reference, which we found the same order of surface stabilities as in our study: $cubic - SiC(111) > cubic - SiC(100) > cubic - SiC(110)$. Since the compration result for cubic-SiC is good agreed with reference. The cohesive energy obitained from PBE, the calculeted value of cohesive energy, -7.21325 eV, is in excellent agreement with the experimental data -7.401 eV in comparision [59]. This result show that zinc-blnede structure is slightly more stable than the wurtzite structure for bulk SiC. That is cohesive energy for wurtzite structure SiC = -7.396 eV [59] and lastly the calculeted value of 3C-SiC for vacancy C-site = 8.733 eV and Si-site = 7.63 eV [60, 61].

Table 3.2: Compartion between calculeted value of Surface energy, cohesive energy and vaccancy energy of SiC in this work and exprimental value by using PBE in abinit code [59, 60, 61].

Indicies	fcc(100)	fcc(110)	fcc(111)	Ecoh(eV/A^2)	Evca(eV/A^2)
This work	0.3169655	0.2277070	0.43674081	-7.21325	8.7833
exp't			0.34300000	-7.401	7.63

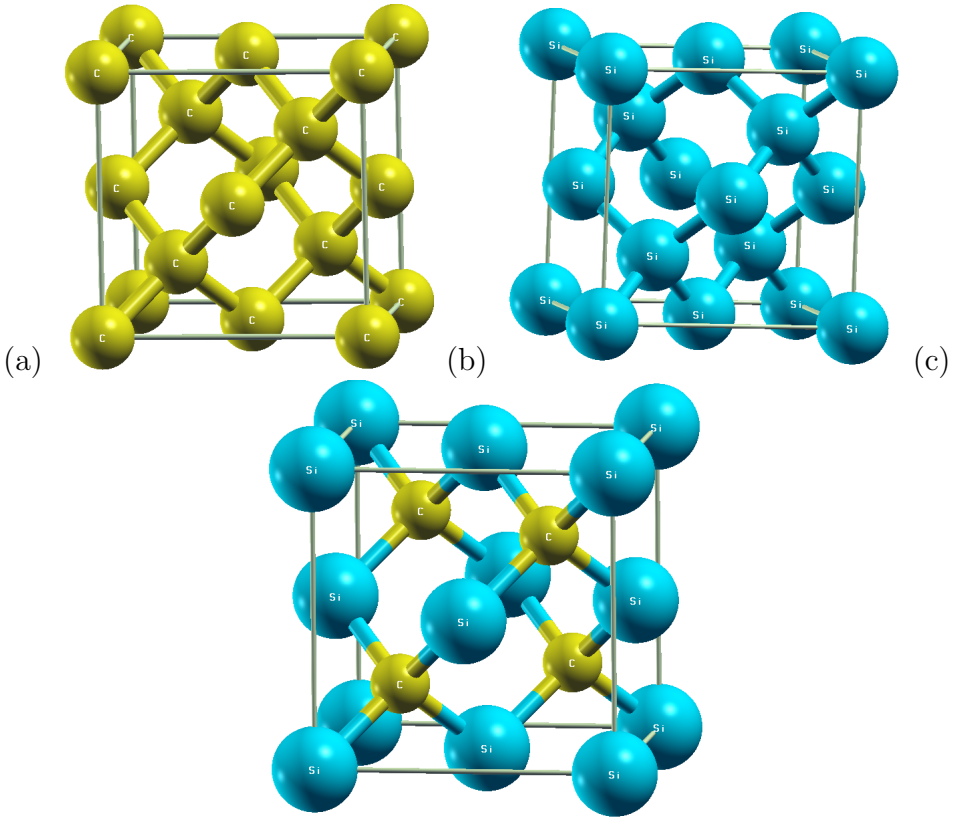

Figure 3.4: Gives Unit cell geometries for (a), Carbon (C) (b), Silicon (Si) and (c), silicon carbide.

3.8 Electronic Band structure of Silicon, Carbon, Silicon-Carbide diamond strcuture

The dispersion curves are shown for wave vectors along a path in the first Brioullin zone. Here, the path is described by the wave vectors Γ, X, M, Γ which are points in the Brioullin zone. The energy of the valence band (VB) at (X) is the highest energy in the VB and is called valence band maximum (VBM). The energy of the conduction band (CB) from (M) is the lowest energy in the CB and is called conduction band minimum (CBM). By using this information, we have calculated band gap energy and discussed as follows.

Table 3.3: The calculated band gap energies for C, Si and SiC were compared with experimental values [60, 61, 62].

symbol	structure	bandgap-type	PBE bandgap	reference
Dimond-C	diamond	indirect	2.66	4.12
si	diamond	indirect	1.09	1.1, 0.58
3C-SiC	zincblend	indirect	2.448	2.36,

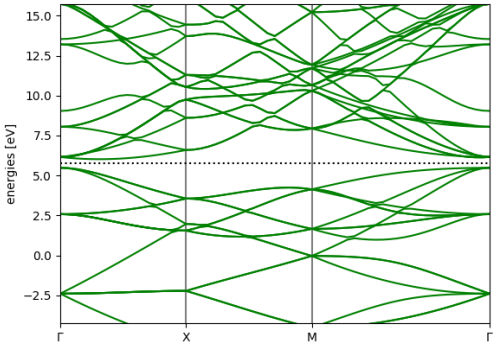

Figure 3.5: Bnadstructure of bulk silicon (Si).

In this figure 3.5, the calculated bandstructure for silicon is given where an indirect band gap between (X) and (M) different (K) point Eg = 1.09 eV which is less than carbon, and greater than exprimental value (0.167) [64], and exactly equal (1.1eV) [62]. Hence showing this material to be has conductor characterized with a completely filled valence bands.
Even if, it is semiconductor. Instead, the band gap energy for an indirect transition for silicon is 0.167 eV [65], and 1.1ev. The band gap energy for direct transitions for silicon is 3.6 eV [66] but silicon can absorbs visible light. Hence, the visible light must excite silicon through indirect transitions. Since conductor can emitt light through zero band gap energy 0 eV. Silicon is a leading semiconductor material [67] and has taken a leading position in semiconductor materials. Therefore, Silicon in diamond structure have significantly weaker bonding between their atoms. This results in a smaller band gap. At room temperature, some of the electrons have enough energy to move into the conduction bands. Meaning that there are some orbitals in the valence band and in the conduction band that hold only one electron. Electrons can travel through the material through these orbitals [68] and Visible radiation produces electron transitions with almost unity quantum efficiency in silicon [69].
Bandgapstructure for carbon(C) in diamond structure is as following figure 3.6.

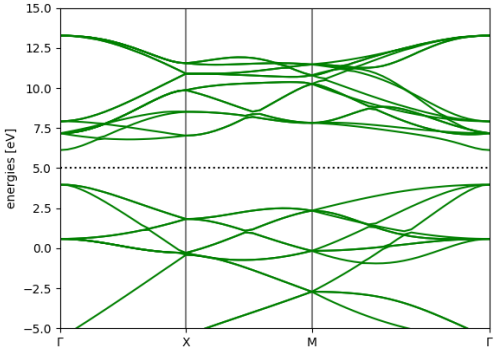

Figure 3.6: Bandstructure of carbon in diamond structure.

Figure 3.6, shows that, the band structure of carbon in Diamond structure, it indicates that the top position of valence band lie on the (X) point, the bottom position of conduction band at (M) point. The indirect bandgap, between (X) and (M) different (K) point Eg = 2.66 eV which is bigger than silicon and less than exeprimental value 4.12 eV [60]. This indicate that, Carbon in diamond structure forms very strong C-C bonds so it has large band gap. Thermal energy available at room temperature is not enough to excite any electrons from the filled band to the empty band. The calculated bandgapstructure of the SiC diamond structure is shown in figure 3.7 below.

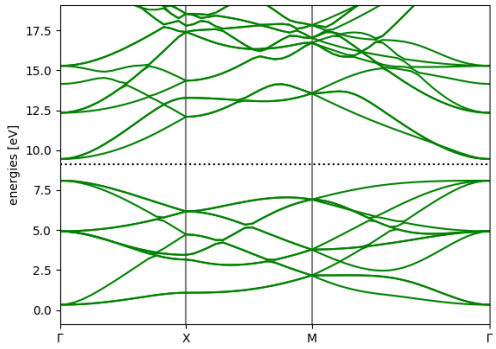

Figure 3.7: Bandstructure of SiC in diamond structures.

From figure 3.7, The bandgap Eg = 2.448 eV, in (SiC) with diamond structure, has small difference comparing to the carbon with diamond structure, and large difference compering to the silicon with diamond structure. This value is larger with comparing to exprimentala value 2.36 eV [62, 63]. It indicates the typical characteristics of bond of the (Si-C) in Diamond structure with indirect band gap. It shows that the top position of valence band lie on the (X) point. The energy of the valence band (VB) is the highest energy. On the (M) point is the lowest energy in the CB and is called conduction band of Brillouin zone. The indirect bandgap, between (X) and (M) different (K) point Eg = 2.448 eV, less than value of (C) and exprimental value with diamond structure and grater than (Si) with diamond structure. This size wide band gap shows that (SiC) in diamond structure to be semiconductor. Beside on this, their fermi-level for silicon, carbon, and silicon-carbide is 12.5 eV, 5.00 eV and 9.10 eV respectively. As a result, the diamond is often considered to be a wide-bandgap semiconductor. The minimal bandgap is indirect, with a value of 2.66 eV for carbon, which can be compared to corresponding values of 0.00 eV for silicon and 2.448 eV for silicon-carbon (SiC), with diamond (fcc) structure, respectively, for the group-IV semiconductors silicon and silicon-carbon (SiC) with diamond structure [68]. Each carbon atom, silicon atom, and silicon-carbon (SiC) atoms in cubic diamond (fcc) contributes four valence electrons to four directional tetrahedral covalent sp^3 bonds linking nearest neighbors. The diamond structure is a good example of strong tetrahedral covalent bonding where the atoms share a valence electron with each neighbor [70].

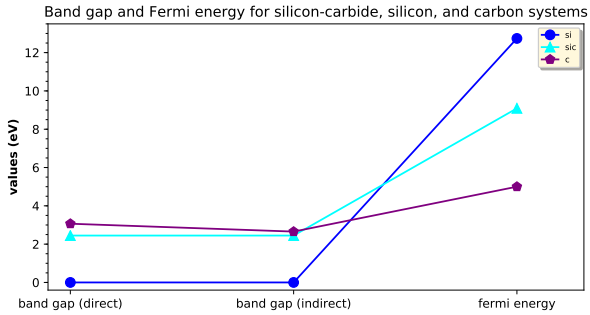

Figure 3.8: Gives bandgap and fermi energy for carbon, silicon, and silicon carbide systems as sammerizied.

3.9 Electronic properties of Silicon Carbide SiC

The chemical bonding of SiC, an individual atom is calculated by the partial DOS and all atoms by the total DOS. Now, we have the correct electronic properties and the total energy of the system per unit cell for SiC. We have calculated the electronic structure of cubic silicon carbide using PBE correlation. Calculation on density of state (DOS) and projected density of state (PDOS) of silicon (Si), carbon (C) and silicon-carbide (SiC) and their corrosponding figures are following.

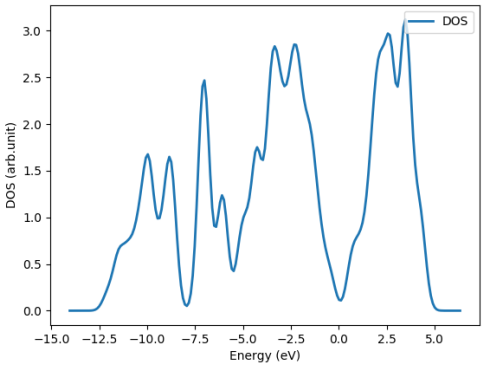

(a) (b)

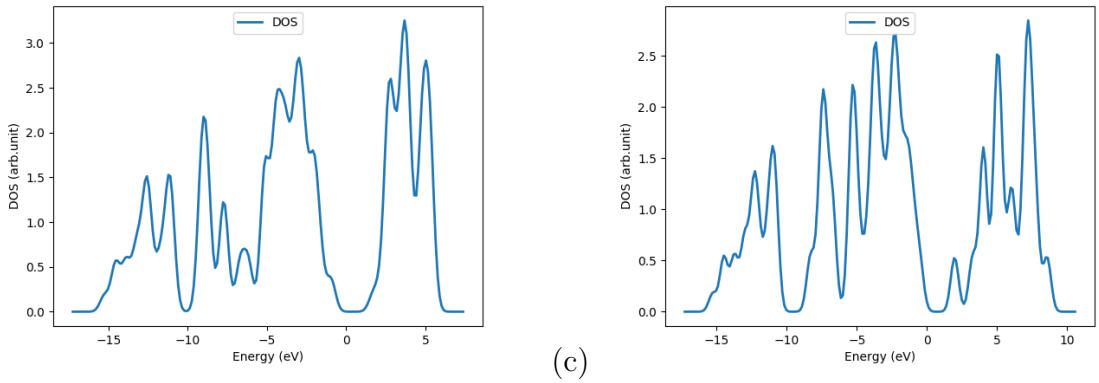

(c)

Figure 3.9: Gives the density of state (DOS) of (a) Silicon(Si), (b) carbon (C) and (c) silicon carbide (SiC)

In this fig 3.9 (a), the low-energy area of Valence band is mainly constituted by (Si 3p, Si 3d) orbital electrons. That is the lower part of valance band ∼4 to ∼5ev(a). And shows narrow, sharp peaks in the DOS, which are mainly composed of the Si-3d orbital. The High-energy area is mainly constituted by (Si 2p and Si 2d) orbital electrons. Figure 3.9 (b), shows the density of state(DOS) of diamond-C. In fig 3.9 (b), the low-energy area of Valence band is mainly constituted by (C 2p and C 2s) orbital electrons. That is the lower part of valence band ∼2.5 to ∼4.75 eV. Figure 3.9(c), shows the density of state (DOS). This figure shows that the lower energy area of valance band mainly constituted by 3d orbital electron. That is the lower part of valance band ∼7.00 to ∼8.75 eV(c). And shows narrow, sharp peaks in the DOS, which are mainly composed of the Si-3d orbital.

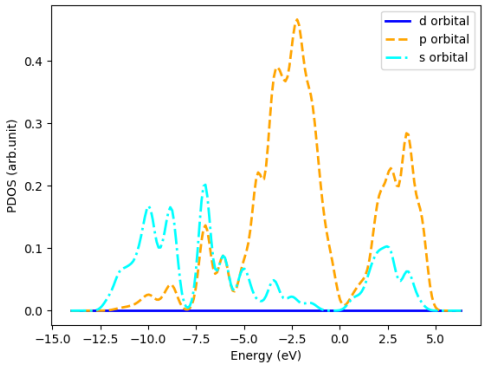

(a) (b)

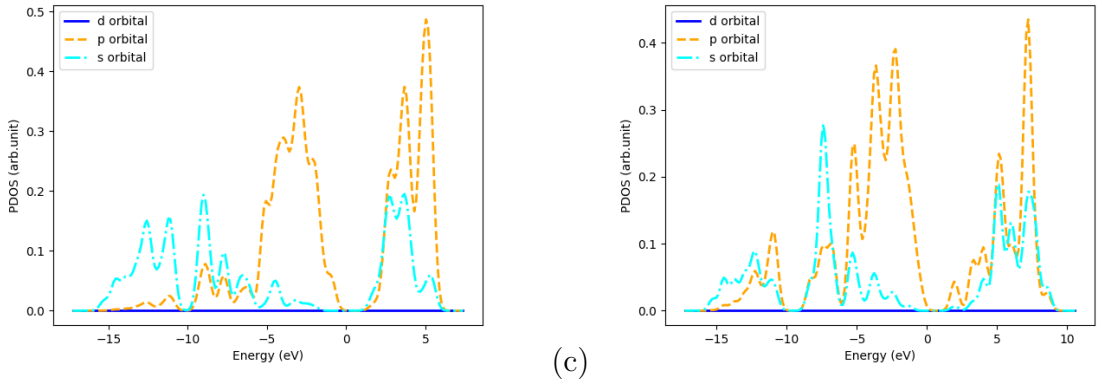

(c)

Figure 3.10: Gives the porjected density of state (PDOS) of (d) Silicon (Si), (e) carbon (C) and (f) silicon carbide (SiC).

In this fig 3.10 (a), the lower part of the valence band at ∼-3.950 eV to ∼0.95 eV (a) and shows narrow, sharp peaks in the PDOS, which are mainly composed of the Si-3p orbital. The upper consists mainly of the Si-3p orbital, where some hybridization of the (Si 3d, Si 3p, c 3s and c 3p) 3p orbitals are located. In this fig 3.10 (b), the lower part of valence band at ∼4.5 eV to ∼7.0eV (b) shows narrow, sharp peaks in PDOS, which are mainly composed of the C-3p orbital. The high-energy area is mainly constituted by (C 2s and C 2p) orbital electrons. In figure 3.10 (c), from top to bottom it listed the projected density of state (PDOS) of silicon and carbon of (Si-C) in diamond structure. The Valence band is composed of two sub bands. That is the lower part of the valence band at ∼6.50 eV to ∼8.5

eV (a) and shows narrow, sharp peaks in the PDOS, which are mainly composed of the Si-3p orbital. The low-energy area is mainly composed of (Si 3p and C 3s) orbital electrons.

3.10 Optical properties of cubic SiC system.

3.10.1 Absorption coefficient

With its wide band gap, high breakdown critical field strength, high electron mobility, and high resistance to radiation, 3C-SiC has a broad range of applications [71]-[76]. As a connection between the transition microscopic physical process of the band and the solid electronic structure, the dielectric function reflects the solid energy band structure and a number of spectral information. Diamond-C, Si, are spacing band gap semiconductors, where as SiC is a direct band gap semiconductor. There for, the optical spectrum of C, Si and SiC are formed by the electron transition among energy levels. Fig 3.11, the optical spectrum of C ,Si, and SiC

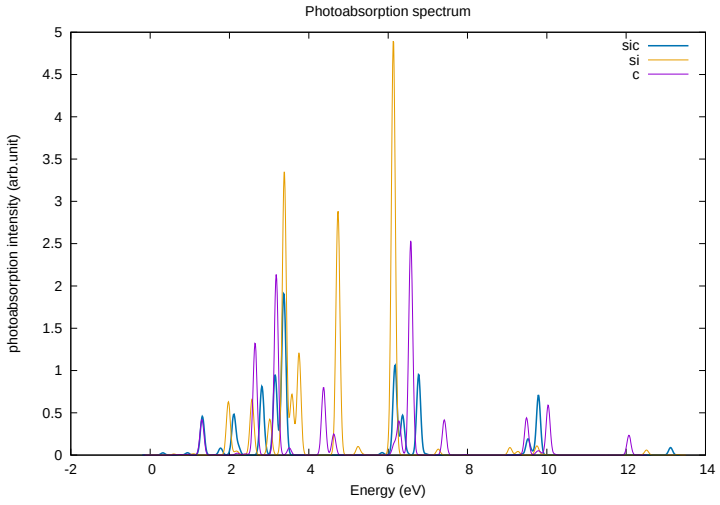

Figure 3.11: The optical spectrum of C ,Si and SiC are formed by the electron transition among energy levels.

are formed by the electron transition among energy levels. In figure 3.11 (rose color), shows that carbon exhibit the absorption largest peak at 6.58040 eV the photon energy level. This indicates that the absorpption is varing from ∼1.5 to ∼ 6.5 eV and increasing rapdily and reachs maximum at 6.58040 eV.
Fig 3.11 (yellow color), the optical spectrum of Si is formed by the electron transition among energy levels. This figure implies that silicon exhibit the largest absorption peaks at 6.13394 eV. And the photoabsorption is increasing from ∼1.9 to 3.45 eV and decreasing from ∼3.46 eV to ∼4.5 eV and also increasing from ∼4.5 eV to ∼6 eV and rapdily reach maximum at 6.13394 eV photon energy.

Fig.3.11 (blue color), the optical spectrum of SiC is formed by the electron transition among energy levels. In figure 3.11(blue color), shows that silicon-carbide exhibit the absorption largest peak at 3.46 eV photon energy. The highest peak value is slightily deviates from exprimental value 1.37 eV [73, 74]. The transition electrons may have been from the C 2p and Si 3p orbits.

3.10.2 Dielectric function

As the thin film thikness decreases, both the real and imaginary parts of the dielectric function decreases significantly and shows a red and black shift. The thin thickness depends on the dielectric function, related to the changes in the interband absorption.

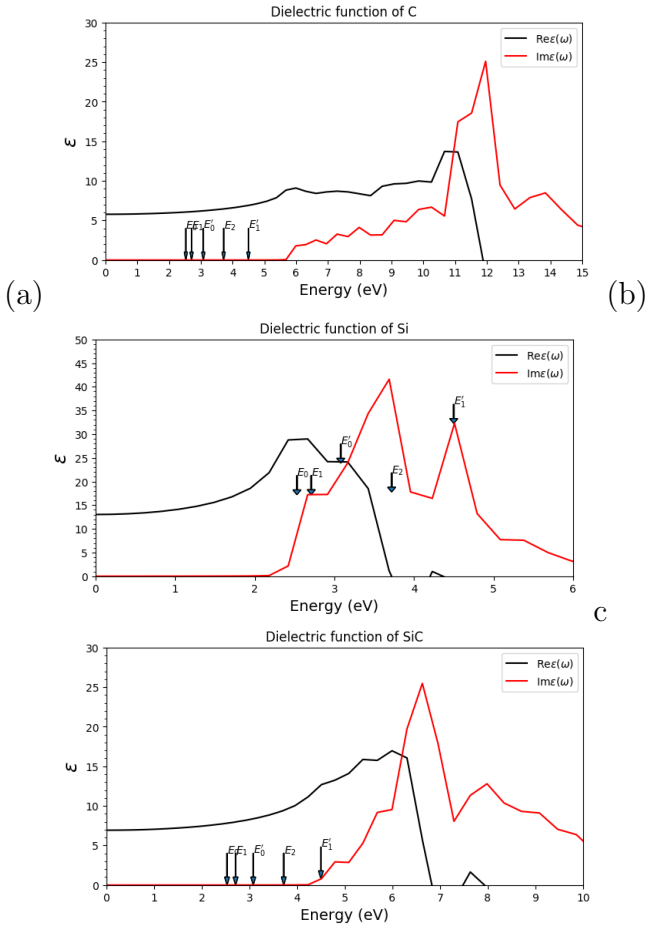

Figure 3.12: Calculated real and imaginary part of the dielectric function for:(a), Carbon (C) (b), silicon (c), silicon carbide (SiC).

In fig 3.12 (a), shows that, carbon exhibit dielectric function of imaginary parts starts from photon energy $\sim$ 5.75 eV. And real part shift dielectric function strat from photon energy value $\sim$ 4.5 eV and then some what increasing slightly up. But fig 3.12(b), shows, silicon exhibit the dielectric function of imaginary parts electron transition silightly shifting up (increasing up) from $\sim$ 2.25 eV to it's maximum peak around$\sim$ 3.5 eV and decreasing down as zigizag form. and real

parts electron transition strat from dielectric function from ∼ 0.5 eV and increasing slowing up to ∼ 3.94 eV and then dicreasing down to dielectric function. In fig 12 (c), shows silicon carbide dielectric function of imaginary parts from ∼4.25eV and increasing up to it's maximum peaks ∼6.75eV and then decreasing imidiately from maximum to ∼7.48 eV and then increasing gradualy up to ∼8eV and aslo decreasing to down. The real parts electron transition of dielectric function start from ∼1eV up to ∼6eV it's maximum peaks and decreasing down to ∼ 6.98eV and become take rest up to ∼7.5eV and the increasing to ∼8eV. In conclusion, a corresponding relation exists among the imaginary parts of the dielectric function, the refractive index, and the adsorption coefficient. Thus, optical properties have a direct relationship with the crystal band and the distribution of electronic DOS. In figure (3.11-3.12), shows that, the optical property of silicon-carbide is directily affected the existance of dielectric constant, absorption and refractive index.

3.10.3 Electron energy loss spectrocopy (EELS).

Electron energy loss spectroscopy (EELS) is the technique to measure the amount of energy loss in an inelastic scattering event, when electrons pass through the material. Transmission electron microscopy (TEM) is the appropriate microscope for EELS since in order to have the projection image, electrons should transport in the material.

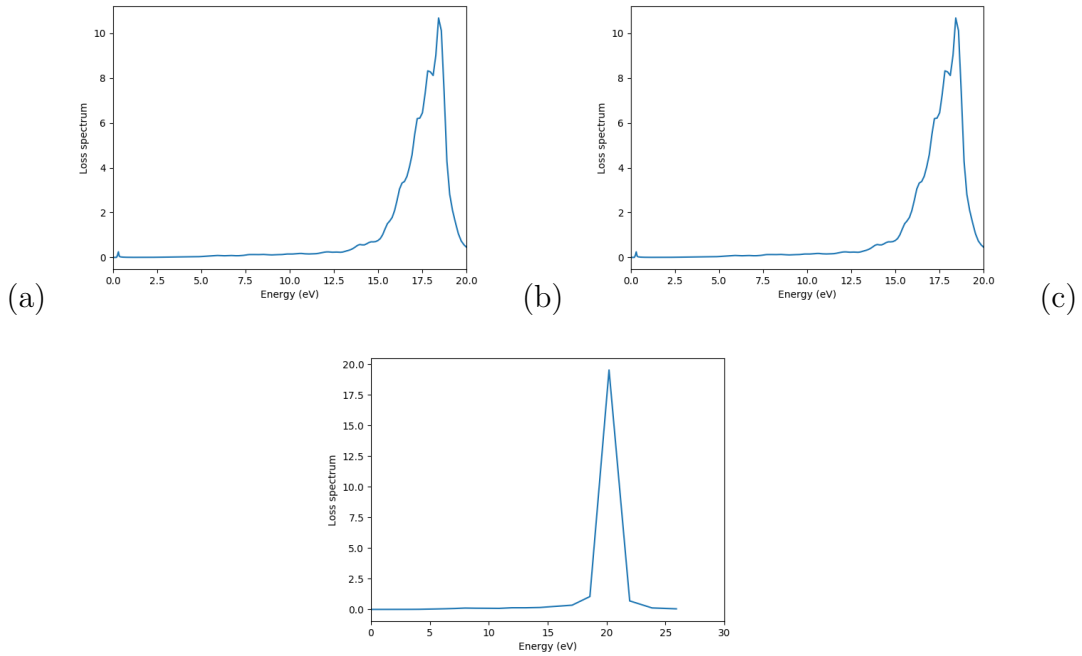

Figure 3.13: Graph of electron energy loss spectron (EELS) for: (a), carbon (b), Silicon (c), Silicon carbide respectively

In figure 3.13 (a and b), show that electron energy loss spectron through carbon and silicon, transmission electron pass through the same energy level that is from ground energy level and gradually increasing electron transport up to maximum peak of 17.5 eV and after riching maximum peak, it dicreasing immiditelly to

downward to ground level energy. In fig 3.13(c), shows, EELS through SiC there is some what no transmission electron passes up to ∼ 16.00eV and after this, electron passes rapidily up to maximum peak between ∼19eV and ∼22.20eV and decreasing energy loss rapidily down ward to ground level. This shows that, SiC material is the appropriate microscope for EELS in order to have the image electron transpot.

3.10.4 Berry phase of silicon, carbon and silicon carbide

Berry phase is polarization expressed in the form of a certain quantum phase. In our system the berry phase corresponding to spontaneous polarization.

Table 3.4: The calculated value spontaneous polarization for bulk carbon (C), bulk silicon (Si) and silicon carbide (SiC).

Bulk structure	PBE value c/m^2	a_0(Å)
Carbon	-4.44×10^{-14}	3.54
Silicon	-6.707 ×10^{-16}	5.44
Silicon carbide	-3.619×10^{-15}	4.38

From table 3.4, shows that the value of polarization in $C = -4.44 \times 10^{-14} C/m^2$ is highest value of that of $SiC = -3.619 \times 10^{-15}$ and $Si = -6.707 \times 10^{-16} C/m^2$. This indicate that at smallest lattice constant value have highest polarization end.

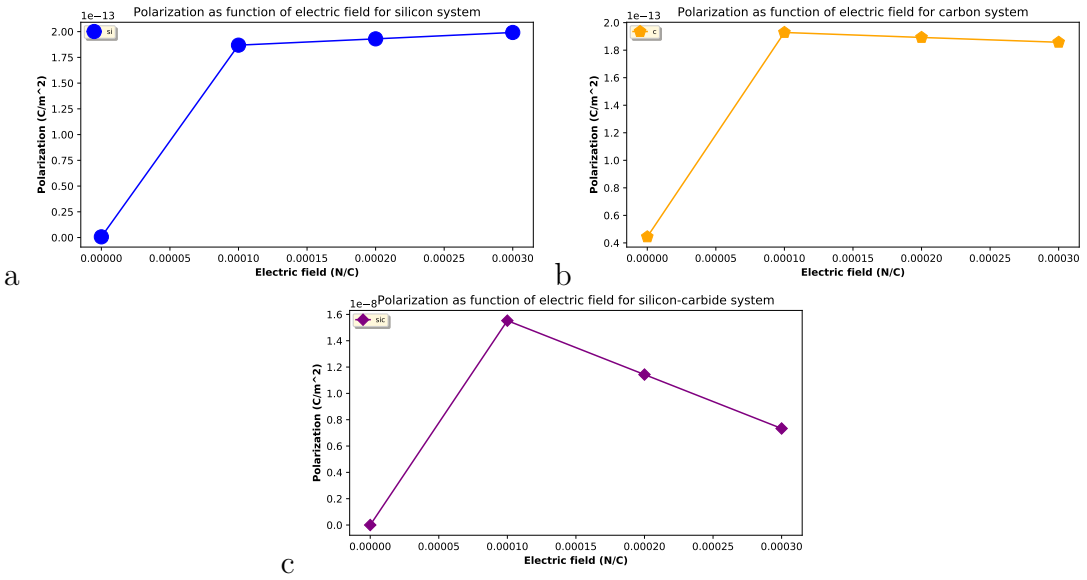

Figure 3.14: Gives polarization as function of electric filed for Si, C, and SiC

In figure 3.14, shows that polarization as function of electric field. From this fig 3.14 (a), the polarizaton effect increasing from the origion to it's maximum point and slightily increasing step to step upto 0.00030 N/C electric filed. In this

case, polarization is affected by electric field direactly or electric field increases, as polarization increases in the silicon atom. In fig 3.14(b), indicates polarization as function of electric field for carbon atom. In this figure, polarization increasing upto it's maximum point of electric field from origin to 0.00010 N/C and dicreasing slightily dowon as field increasing the range. In fig3.14(c), silicon carbide exhibit polarization as function of electric field. In this figure, polarization increasing imidetily upto it's maximum peak to 0.00010 N/C and dicreasing straightly down ward with out any step.

3.11 Workfunction of Carbon, Silicon and Silicon-Carbide in diamond structures.

The atoms or electrons are located at the minimum of the potential. The work function is given by the difference between the Fermi level and the vacuum level [43]. The calculated value of workfunction for bulk silicon (bulk-Si), bulk carbon (bulk-C), bulk silicon carbide (bulk-SiC) and aslo workfunction for their different indices fcc(100, 110, 111) are discussed in table 3.5 and corresponding graphs as follows. Generally, the calculated value for diamond silicon, carbon, and bulk silicon carbide in their bandstructures are in table 3.5.

Table 3.5: The calculated value of workfunction of bulk and diamond silicon, carbon, and silicon carbide in thier bandstructures.

Structural properties	C(diamond)	Si(diamond)	SiC(diamond)
Bandgap energyin (eV)	2.66	0.00	2.446
Fermi-level in (eV)	5.00	12.75	9.10
Bulk workfunction in (eV)	-13.36	-20.13	-16.54
workfunction in (eV) (100)	6.80	4.11	5.84
workfunction in(eV) (110)	6.00	3.57	3.96
workfunction in(eV) (111)	6.93	4.43	6.10

Accorrding to our data calculeted by DFT in table 3.5 we drown the following discussion by graphicaly. Graph of workfunction of bulk silicon, carbon, SiC at ground level or in zero bundary and periodic boundary condition.

In figure 3.15 are gives the workfunction of (a) bulk silicon (Si),(b) bulk carbon (C), (c) bulk silicon carbide (SiC) in zero bundary condition. In figure 3.15(a, b and c) indicates average effective potential of Si, C and SiC at 4.5 eV, -10 eV and -7.5 eV respectively.
In figure 3.16 are gives workfunction of(d) Si (100), (e) C (100) and (f) SiC (100) in periodic boundary condition and shows that the average effective potential between $\sim$ 10.5 eV to $\sim$ -10.5 eV, $\sim$ 9.75 eV to $\sim$ -9.75 eV and 10 eV to -9.75 eV respectively.
In figure 3.17 are gives workfunction of(g) Si (110), (h) C (110) and (i) SiC (110) in periodic boundary condition and indicate the average effective potentials are between 12.5 eV to -14 eV, 8 eV to -17.5 eV and 9 eV to -15 eV respectively.

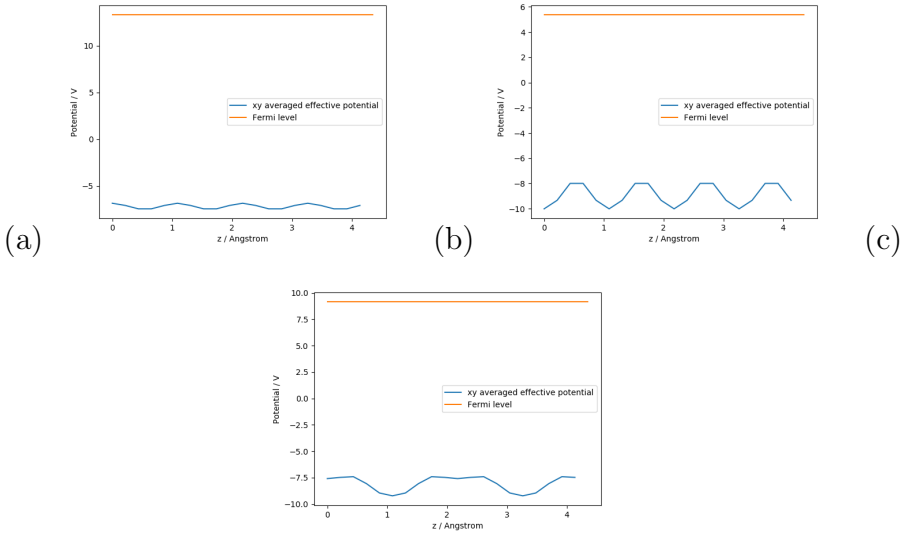

Figure 3.15: workfunction of bulk silicon (Si), bulk carbon (C), bulk silicon carbide (SiC).

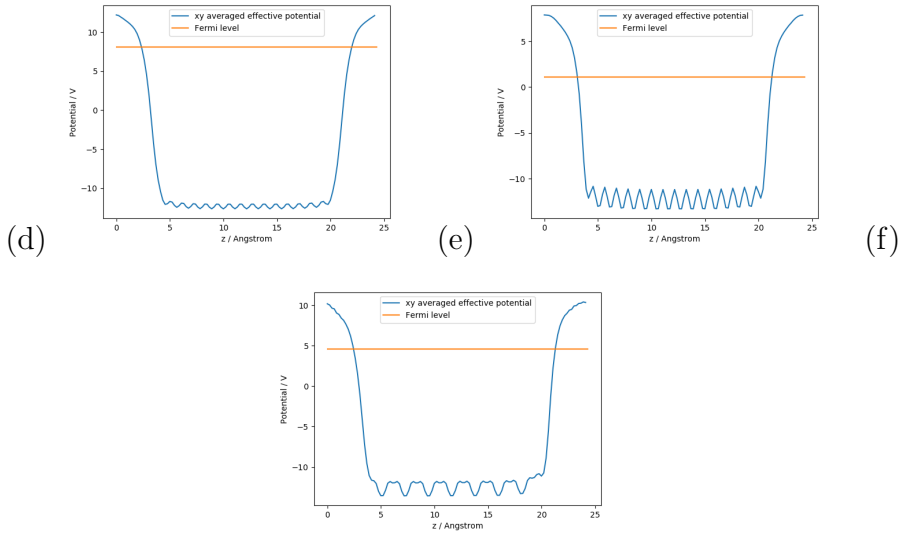

Figure 3.16: workfunction of silicon (Si(100)), carbon (C(100)), silicon carbide (SiC(100)) in periodic boundary condition.

Lastly in figure 3.18 (j, k, and l) are gives workfunction of (j) Si (111), (k) C (111) and (l) SiC (111) in periodic boundary condition and indicates average effective potentails between 10 eV to 23.5 eV, 8 eV to 23.75 eV and 9 eV to 23.75 eV respectively. In figure:3.18, the blue line is the xy-averaged potential (electrostatic potential) and the red line is the fermi-level.

In fig 3.19 indicate, that the summariezed value of work function for bulk and structural system for carbon, silicon and silicon carbide system.

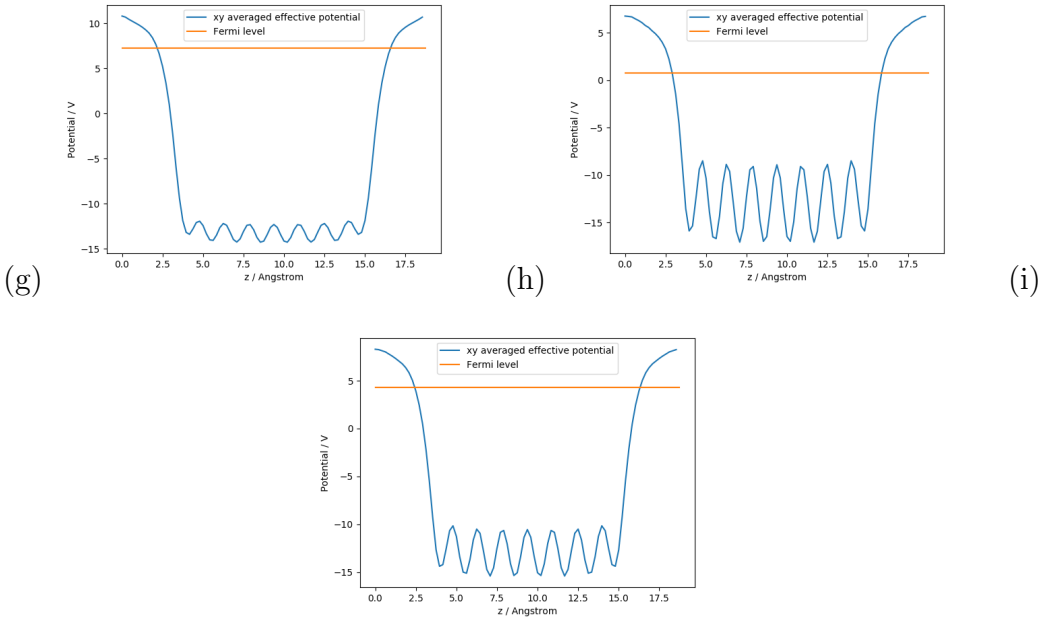

Figure 3.17: workfunction of silicon (Si(110)), carbon (C(110)), silicon carbide (SiC(110)) in periodic boundary condition.

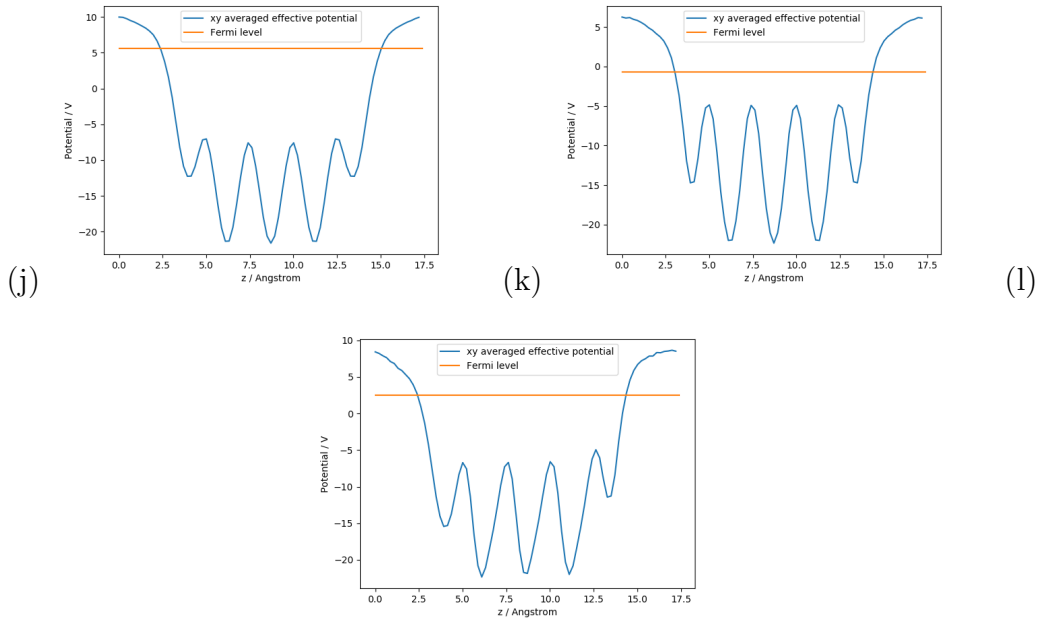

Figure 3.18: workfunction of silicon (Si (111)), carbon (C (111)), silicon carbide (SiC (111)) in periodic boundary condition.

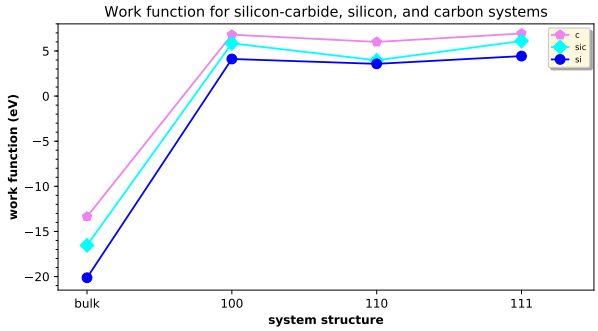

Figure 3.19: Gives work function for silicon carbide, silicon and carbon system.

3.12 Monte Carlo methods

3.12.1 Electron transport in cubic silicon carbide.

The Monte Carlo method for electron transport is a semiclassical Monte Carlo(MC) approach of modeling semiconductor transport. Electron transport system for carbon, silicon and silicon carbide reperesnted in figure by using Green function as follows. In figure 3.20, shows, electron transport in carbon, silicon and silicon

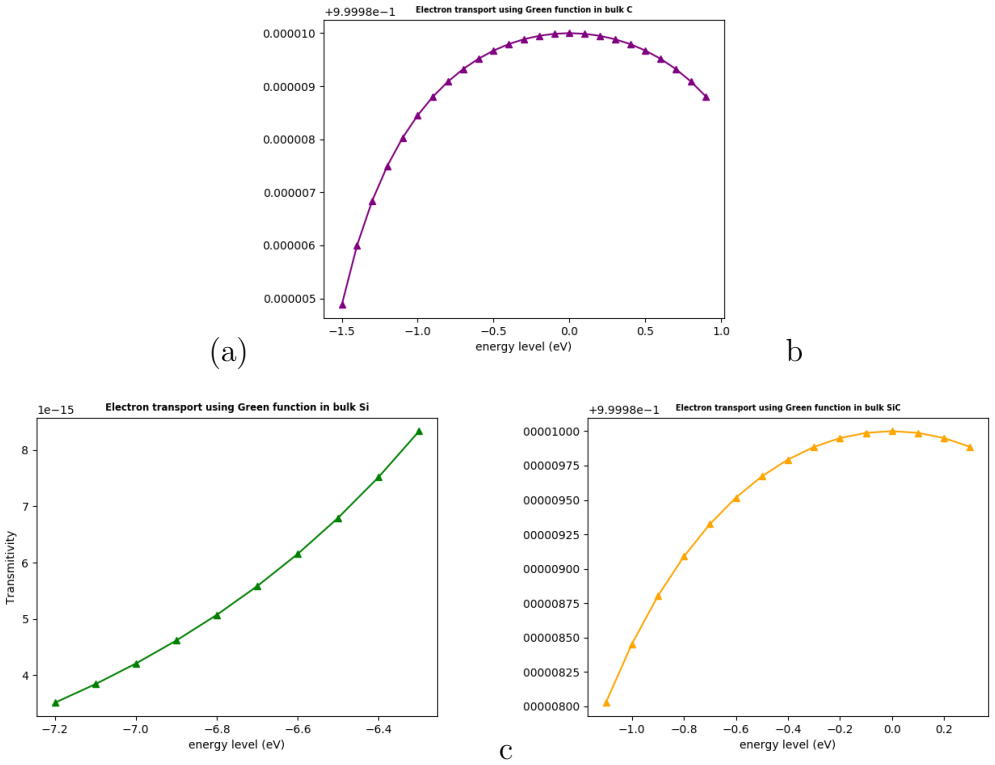

Figure 3.20: Gives energy vs transmitivity value of electron transport for (a), cubic carbon (b), cubic silicon and (c), cubic silicon carbide systems.

carbide system.
In this figure 3.20(a), the transmision of electron strat from ground level to 1.0 or

0 to 1.0eV transmision maximum point in negative transition junction or barrier. In fig 3.20(b), the transmision of electron strat from $\sim -7.2to - 6.58eV$ the energy level for silicon and In fig 3.20(c), shows transmision of electron strart from $\sim -2.2eVto2.2eV$ the energy level for silicon carbide(SiC) as open parabolic path downward.

3.12.2 Monte Carlo method as hopping or jumping

Monte Carlo methods, coupled with so-called transition-state methods guiding the selection of reasonable Monte Carlo steps, appear to be promising. Acording to this state, the electron transport in silicon carbide system can repersnted as following figure 3.21. In fig 3.21 (a), shows that, the transition state of electron

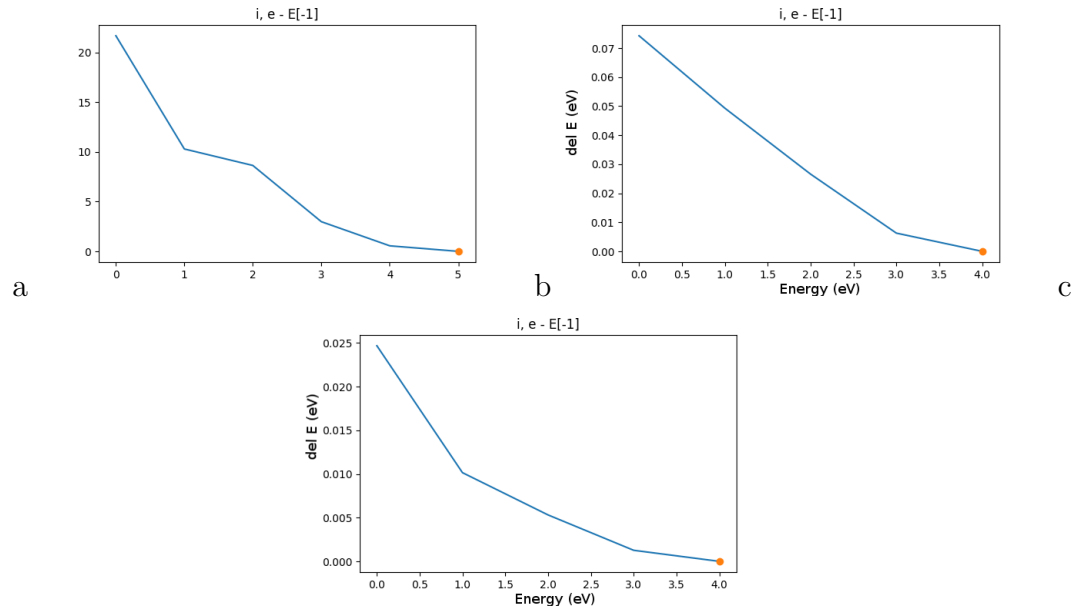

a b c

Figure 3.21: Gives Minimum hoppinng of electron transport in energy levels (a), carbon, (b), silicon, (c), silicon carbide

in carbon strat from the length zero to $\sim$ 5 eV and hopping the electron step-by-step as zigizag manner. i.e between 0 to 1, hopping stright down and take some rest. And 1 to 2, 3 to 4, 4 to 5 eV rich the gronud level. In fig (b), shows that, the transition state of electron in silicon transite in very small intreval which compering with the length of carbon atoms. In this case, the transition state electron take the between 0 to 4 eV. The electron hopping coming down 0 to 3 eV and take the rest at some instant of time, then dicreasing solow dowm up to 4 eV. In fig 3.21 (c) shows that, the transition state of electron in silicon carbide. In this fig 3.21(c), the hopping of electron transite step-by-step but it hopping from 0 to 1, then 1 to 3, and 3 to 4 ev. This indicate that silicon carbide transmition of electrons are midium.There for,silicon carbide is very important structure for today's nanotechonology.

Chapter 4

Conclusion

- In this paper, we studied electron transport in silicon carbide as DFT and MC methods in abinit code by PBE or GGA approximation with in FHI psudopotential.
- Therefor, Energies as a function of volume for SiC in bulk structure to obtaind lattice constant, bulk modulus, kpts and cut-off energy and also varoius energy such as surface energy in different indices, cohesive energy and vaccancy energy were performed with GGA approximation and PBE correlation.
- Combined with the results from other calculated works and experimental data.
- We studied various electronic and physical properties of the systems involving carbon, silicon and silicon carbide in bulk structure. We utilised the GGA pseudopotential in a methodology based on the plane wave approach.
- The ABINIT simulation packages developed were used to perform the calculations.
- Our results were compared with previous theoretical and experimental results which were available. Interestingly our results within the GGA are close to the experimental data. When compared to the other work where PBE was employed.
- The equlibrium lattice constant value callculeted for SiC bulk structures are in execellent agreement for PBE (4.38 Å) compered to reported exeprimental data.
- The bulk modulus obtained from PBE, is very closely agree value with comparision to the exprimental one (202 Gpa).
- K-point convergence of SiC was analysed in the unit cell by varying the Monkhorst-Pack gird the calculeted value for SiC in PBE yileds by using simulation in abinit code is 4x4x4.
- The fhi(Fritz-Haber-Institute) was used to perform the total energy calculations within the pseudopotential framework for all systems.

- In our system the calculated value for SiC by simulation in abinit code with PBE, the cut off energy of the plane wave is set to be 400 eV. This shows that our systems is very good agreed estimation reliable results.
- The PBE overcome the DFT bandgap underestimation, and provides more accurate approximation. The bandgaps calculated for 3C-SiC with this method is in good agreement with the experimental results.
- The Monte Carlo simulations of electron transport, the simulated electron is placed at the conduction band minimum.
- Since the (SiC) with bulk structure is an existing experimental structure, our results shows that this structure has an interesting physical and electrical properties and has important application for today's techonology.

Bibliography

[1] E. G. Acheson, *Production of Artificial Crystalline Carbonaceous Materials* (US, 1893).

[2] Shubert and E. Fred, Light-Emitting Diodes (Cambridge University Press, 2003).

[3] K. Jarrendahl and R. F. Davis, *SiC Materials and Devices*. (Academic Press, London, 1998).

[4] Tairov, Y. M. Vodakov and Y. A. *Group IV Materials (Mainly SiC)*, Topics in Applied Physics, JI. Pankove ed. (Springer-Verlag Berlin Heidelberg, 1977).

[5] Carl-Mikael Zetterling, *Process technology for Silicon Carbide devices*; INSPEC, (London, 2002).

[6] T. Burke, K. Xie, J. R. Flemish, R. Singh, T. Podlesak and J. H. Zhao, *Silicon Carbide Power Devices for High Temperature, High Power Density Switching Applications*, (Proceedings of the Twenty-Second International Power Modulator Symposium, 1996).

[7] R.C. Clarke and J.W. Palmour, *SiC Microwave Power Technologies*, Proc. IEEE **90**, 987-992 (2002).

[8] K. Jarrendahl and R. F. Davis, *SiC Materials and Devices*. (Academic Press, London, 1998).

[9] Gryko et al., *Low-density framework form of crystalline silicon with a wide optical band gap Phys*. Rev. B **62**, (2000)

[10] M. B. J. Wijesundara and R. G. Azevedo, *Silicon Carbide Microsystems for Harsh Enviroments*. (Springer New York, 2011).

[11] S. E. Saddow, *Silicon Carbide materials for biomedical applications and Silicon Carbide Biotechnology A Biocompatible Semiconductor for Advanced Biomedical Devices and Applications*, (Elsevier Inc. p.**1-15**, 2012).

[12] Online reading Crystal structure http://www.youtube.com/(lastupdate).

[13] H. Morkoc, S. Strite, G. B. Gao, M. E. Lin and B. Sverdlov et al. *Large band gap SiC, IIIV nitride, and IIVI Zn Sebased semiconductor device technologies* Journal of Applied Physics, **76**, 1363, (1994).

[14] Murnaghan, and F. D. *The Compressibility of Media under Extreme Pressures*. (Proceedings of the National Academy of Sciences of the United States of America. 1944).

[15] S. Potbhare, N. Goldsman and A. Lelis, *Modeling and Characterization of a 4H-SiC DMOSFET*, San Francisco, (CA, 2008).

[16] Burke, K. Xie, J. R. Flemish, R. Singh, T. Podlesak, and J. H. Zhao, *Silicon Carbide Power Devices for High Temperature, High Power Density Switching Applications* (Proceedings of the Twenty-Second International Power Modulator Symposium, 1996).

[17] W. Wesch, *Nucl. Instrum. Methods Phys. Res.* B**116**, 305 (1996).

[18] P. Neudeck, *J. Electron. Mater.* **24**, 283 (1995).

[19] G. Pensl, M. Bassler, F. Ciobanu, V. Afanasev, H. Yano, T. Kimoto, and H. Matsunami, (MRS Proc. 640 (2000).

[20] KṠarasamak, S. Limpijumnong, W. R. L. Lambrecht, *Computational Materials Science* **49** S43-S46 (2010).

[21] V. Tilak, K. Matocha and G. Dunne *Interface Trap and Mobility Characterization of Silicon Carbide MOSFET Inversion Layers* (Materials Science Forum, 616-617, 2009).

[22] S. Potbhare, N. Goldsman, A. Akturk, M. Gurfinkel, A. Lelis, and J. Suehle *Energy- and Time Occupation*.

[23] J. P. Perdew K. Burke and M. Ernzerhof, *Phys. Rev. Lett.* **77** (1996) 3865,17,38,70.

[24] X. Gonze, J. M. Beuken, R. Caracas, F. Detraux, M. Fuchs, G. M. Rignanese, L. Sindic M. Verstraete G. Zerah F. Jollet M. Torrent, A. Roy M. Mikami Ph Ghosez J. Y. Raty and D. C. Allan, *Computational Material Science* **25** 478 (2002).

[25] R. Car, and M. Parrinello, *Phys. Rev. Lett.* **55**, 2471 (1985).

[26] M. Parrinello and A. Rahman, *J. Appl. Phys.* **52**, 7182 (1982).

[27] Gian-Marco Rignanese *DFT in the abinit code* May 26 to June 6, (2014).

[28] J. Kohanoff and N. I. Gidopoulos, and Stephen Wilson *Density Functional Theory: Basics, New Trends and Applications;* **2***, Part 5, Chapter 26, and Handbook of Molecular Physics and Quantum Chemistry*; Stephen Wilson, and John Wiley and Sons, (Ltd, Chichester, 2003).

[29] P. Hohnberg and W. Kohn, *phys. Rev.* **136**, 3B (1964).

[30] W. Kohn and L. J. Sham, *Phys. Rev.* **140**, 1133A (1965).

[31] K. N. Nigussa (PhD), *Analysis with Density Functional Theory calculation*, (AAU, 2018).

[32] notes provided, and there by cited-in literatures.

[33] R. W. Shaw and W. A. Harrison, *Phys. Rev.* **163**, 604 (1967).

[34] D. R. Hamann, M. Schlüter and C. Chiang, *Phys. Rev. Lett.* **43**, 1494 (1979).

[35] Murnaghan and F. D. *The Compressibility of Media under Extreme Pressures.* (Proceedings of the National Academy of Sciences of the United States of America. 1944).

[36] Birch and Francis *Finite Elastic Strain of Cubic Crystals. Physical Review.* **71** (11): 809-824 (1947).

[37] Bloch's Theorem-Durham University https://www. researchgate. net/ (lastupdated).

[38] H. J. Monkhorst and J. D. Pack *Special points for Brillouin-Zone*; Physical Review B, **13, 12**, 5188-5192, (1976).

[39] D. Vanderbilt, *Phys. Rev. B.***41**, 7892 (1990).

[40] Online surface energy reading https://www. researchgate. net/ (lastupdated, December 2011)

[41] W. F. Egelhoff. *Core-level binding-energy shifts at surfaces and in solids. Surface Science Reports*, **6, 6-8**, 253 - 415, (1987).

[42] Shrader, D., I. Szlufarska, and D. Morgan, *Cs diffusion in cubic silicon carbide*. Journal of Nuclear Materials, **421** 89-96 (2012).

[43] Binggeli, N. Fall, C. J. and Baldereschi *A. Deriving accurate work functions from thin-slab calculations. J.Phys.Condens.Matter* **11**, 2689-2696, (1999).

[44] Yue P. and Yintang Y. (Science Press. 2000).

[45] CoorsTek, *SiC-optical-brochure.pdf*. (lastupdated,2017)

[46] R. F. Egerton, *Electron Energy-Loss Spectroscopy in the Electron Microscope, 3 Edition*, (Springer, 2011.)

[47] V. J. Keast, *Ab initio calculations of plasmons and interband transitions in the low-loss electron energy-loss spectrum, J. Electron. Spectrosc. Relat. Phenom.***143** (2005) 97-104.

[48] V. P. Oleshko, M. Murayama, and J. M. Howe, *Use of Plasmon Spectroscopy to Evaluate the Mechanical Properties of Materials at the Nanoscale, Microsc. Microanal.***8** (2002) 350-364.

[49] P. Hovington, D. Drouin, and R. Gauvin, CASINO: *A New Monte Carlo Code in C Language for Electron Beam Interaction - Part I: Description of the Program*, Scanning, **19** 1-14. (1997)

[50] C. Fiolhais, F. Nogueira, and M. Marques; *A Primer in Denisty Funational Theory* (Speinger, 2003).

[51] Online bad-gap reading https://en.wikipedia.org/wiki/band-gap. (last edited on 11, December, 2019).

[52] A. Ferretti, A. Calzolari, B. Bonferroni, and R. Di Felice. J. Phys. *Condens. Matter*, **19**, 036215, (2007)

[53] A. P. Sutton *Electronic Structure of Materials*; (Oxford Science Publications, 1993).

[54] John P. Perdew, Kieron Burke, and Matthias Ernzerhof *Generalized Gradient Approximation Made Simple*; Physical Review **77, 18**, 3865-3868, (1996).

[55] R. Gauvin, E. Lifshin, H. Demers, P. Horny, and H. Campbell, *A New Monte Carlo Program that Computes X-ray Spectra Obtained with a Scanning Electron Microscope*, and Microsc. Microanal. **12** 49-64 (2006).

[56] online lattice constant reading https://pdfs.semanticscholar.org/.

[57] Murnaghan, and F. D. *The Compressibility of Media under Extreme Pressures*. (Proceedings of the National Academy of Sciences of the United States of America. 1944).

[58] Stefan Kurth, and John P. Perdew; *Role of the exchange-correlation energy: Nature's glue*; International Journal of Quantum Chemistry; **77**, **5**, 814-818 (2000).

[59] *Online surface energy reading* https://www.researchgate.net/.

[60] *Online cohesive energy* https://www.scienomics.com/.

[61] *online vaccancy energy reading* https://ec.europa.eu/research/ *industrial-technologies/modelling-materials-en.html*.

[62] *Online reading* https://www.iosrjornals.org/.

[63] https://www.britannica.com/*science/electricity/photoelectric-condctivity/*. (online).

[64] *Online reading* https:// www. ioffe, run/SVA/NSM/ semicond/SiC/ (lastupdated).

[65] G. L. Harris (Hrsg.), *Properties of Silicon Carbide*, EMIS Data review Series **13**, INSPE, (1995).

[66] Prof. Pat. Sh. (2012). *Elemental Carbon, Silicon, Germanium. (online)*. http://butane.chem.uiuc.edu (lastupdated: Dec, 2014).

[67] P. A. Ivanov and V. E. Chelnokov, *Semicond. Sci. Technol.* **7**, 863 (1992).

[68] *Online badgap reading* https://en.wikipedia.org/wiki/bandgap.

[69] A. Lee, H. Liu, *A. Seeds, Semiconductor Science and Technology* **28** 015027-015037. (2013).

[70] Prof. Pat. Sh. (2012). *Elemental Carbon, Silicon, Germanium. (online).* https://butane.chem.uiuc.edu. (lastupdated, Dec, 2014).

[71] Micha and l. Po. *Electronic Properties of Single Crystal CVD Diamond and its Suitability for Particle Detection in Hadron Physics Experiments*. (Universit atin Frankfurt am Main, 2008).

[72] Richard. Ch. Andrew. *First principles studies of Si-C alloys. Department of Physics*, (University of Pretoria, FE, 2013).

[73] V. V. S. S. Srikanth, X. Jiang, and A. Köpf, *Surface and Coatings Technology* **204** 2362-2367. (2010)

[74] T. Ito, T. Akiyama and K. Nakamura, *Journal of Crystal Growth* **362** 207-210, (2013).

[75] *Online reading material properties and comparetion chart* /top-Seiko.com/.

[76] R. Chimata, Optical Properties of Materials Calculated from First Principles Theory, (Uppsala Universitet, 2010).

DECLARATION

ADDIS ABABA UNIVERSITY
COLLEGE OF NATURAL AND COMPUTATIONAL SCIENCES
DEPARTMENT OF PHYSICS

MSc Thesis:
Electron transport in SiC system.

Name of Candidate: Roba Chukalo

I the under signed declare that the thesis is my original work and no part of it can be claimed as an intellectual property of anybody else except me and my advisors.

Signature: _____
e-mail:chukaloroba@gmail.com

Place and time of submission:
Addis Ababa University
Department of Physics
Jaunary, 2020.

This thesis has been submitted for examination with my approval as University advisor.

signature: _____
e-mail: _____